



**UNIVERSITY OF LEEDS**

This is a repository copy of *Abscisic acid receptors functionally converge across 500 million years of land plant evolution.*

White Rose Research Online URL for this paper:

<https://eprints.whiterose.ac.uk/222614/>

Version: Accepted Version

---

**Article:**

Zimran, G., Shpilman, M., Hobson, E. et al. (13 more authors) (2025) Abscisic acid receptors functionally converge across 500 million years of land plant evolution. *Current Biology*. ISSN 0960-9822

<https://doi.org/10.1016/j.cub.2024.12.043>

---

This is an author produced version of an article published in *Current Biology*, made available under the terms of the Creative Commons Attribution License (CC-BY), which permits unrestricted use, distribution and reproduction in any medium, provided the original work is properly cited.

**Reuse**

This article is distributed under the terms of the Creative Commons Attribution (CC BY) licence. This licence allows you to distribute, remix, tweak, and build upon the work, even commercially, as long as you credit the authors for the original work. More information and the full terms of the licence here:

<https://creativecommons.org/licenses/>

**Takedown**

If you consider content in White Rose Research Online to be in breach of UK law, please notify us by emailing [eprints@whiterose.ac.uk](mailto:eprints@whiterose.ac.uk) including the URL of the record and the reason for the withdrawal request.



[eprints@whiterose.ac.uk](mailto:eprints@whiterose.ac.uk)  
<https://eprints.whiterose.ac.uk/>

## Main Manuscript for

# Abscisic acid receptors functionally converge across 500 million years of land plant evolution.

Gil Zimran<sup>2</sup>, Michal Shpilman<sup>2</sup>, Eve Hobson<sup>3</sup>, Yasuko Kamisugi<sup>3</sup>, Amichai Baichman-Kass<sup>2</sup>, Hong Zhang<sup>1</sup>, Rafa Ruiz-Partida<sup>4</sup>, María R. González-Bermúdez<sup>4</sup>, Matan Azar<sup>2</sup>, Erez Feuer<sup>2</sup>, Maayan Gal<sup>5</sup>, Jorge Lozano-Juste<sup>4</sup>, Jan de Vries<sup>6,7,8</sup>, Andrew C. Cuming<sup>3</sup>, Assaf Mosquna<sup>2\*</sup> and Yufei Sun<sup>1\*</sup>.

### Affiliations:

1. School of Agriculture and Biotechnology, Shenzhen Campus of Sun Yat-sen University, Shenzhen, China
  2. The Robert H. Smith Institute of Plant Sciences and Genetics in Agriculture, the Hebrew University of Jerusalem, Rehovot 7610000, Israel
  3. Centre for Plant Sciences, Faculty of Biological Sciences, University of Leeds, Leeds LS2 9JT, United Kingdom
  4. Instituto de Biología Molecular y Celular de Plantas (IBMCP), Universitat Politècnica de València (UPV), Consejo Superior de Investigaciones Científicas (CSIC), 46022, Valencia, Spain
  5. Department of Oral Biology, The Maurice and Gabriela Goldschleger School of Dental Medicine, Sackler Faculty of Medicine, Tel Aviv University, Tel Aviv, Israel
  6. University of Goettingen, Institute for Microbiology and Genetics, Department of Applied Bioinformatics, Goldschmidtstr. 1, 37077 Goettingen, Germany
  7. University of Goettingen, Campus Institute Data Science (CIDAS), Goldschmidtstr. 1, 37077 Goettingen, Germany
  8. University of Goettingen, Goettingen Center for Molecular Biosciences (GZMB), Department of Applied Bioinformatics, Goldschmidtstr. 1, 37077 Goettingen, Germany
- \*Corresponding authors: Assaf Mosquna and Yufei Sun

Email:

assaf.mosquna@mail.huji.ac.il, sunyf37@mail.sysu.edu.cn

### ORCID:

Gil Zimran, 0009-0009-8735-0014  
Michal Shpilman, 0009-0000-7336-7979  
Eve Hobson, 0009-0002-0317-3321  
Yasuko Kamisugi, 0000-0002-5265-3658  
María R. González-Bermúdez, 0000-0002-1853-6781  
Amichai Baichman-Kass, 0000-0003-0924-3191  
Matan Azar, 0009-0004-9208-3241  
Erez Feuer, 0000-0002-7748-4504  
Jorge Lozano-Juste, 0000-0001-7034-566X  
Jan de Vries, 0000-0003-3507-5195  
Andrew C. Cuming, 0000-0003-2562-2052  
Assaf Mosquna, 0000-0003-3507-5195  
Yufei Sun, 0000-0002-5016-6848

**Author Contributions:** G.Z., A.C.C., J.d.V., A.M., and Y.S. designed the experiments. G.Z., Y.S., and A.B.K. performed sequence variation analysis. M.S., G.Z., H.Z. and Y.S. conducted the phosphatase assays. M.A. and E.F. helped with the genetic analyses of the Arabidopsis plants. A.C.C., E.H and Y.K preformed the moss genetic analysis. R.R.P., M.R.G.B., and J.L.J. solved the oligomeric state of the proteins. Y.S. and M.G. performed and analyzed the ITC experiments. A.M., Y.S., A.C.C., J.d.V. and J.L.J. supervised experiments. G.Z., A.C.C., J.d.V., A.M., and Y.S. drafted the manuscript, with contributions from all co-authors.

# Summary

Abscisic acid (ABA) functions as a central regulator of dehydration responses in land plants. As such, ABA signaling was pivotal in facilitating the colonization of terrestrial habitats. The conserved ABA signal transduction module consists of 2C-type protein phosphatases (PP2Cs) and their ABA-triggered inhibitors, PYRABACTIN RESISTANCE 1-like proteins (PYLs). Recent evidence indicates that ABA perception emerged from a latent signaling pathway involving a constitutively PP2C-inhibiting PYL homolog. Consequently, ancestral ABA receptors exerted high background signaling, limiting the dynamic range of ABA-dependent signaling. In angiosperms, ABA receptor families are characteristically large and diverse and include a clade-specific subgroup whose members form homodimers, thereby assuming strict ABA dependency. Here, we show that ABA receptors in the mosses originate from an independent expansion, giving rise to three subfamilies. Yeast two-hybrid and *in vitro* PP2C-inhibition assays indicate that moss PYLs feature low basal activities. However, size exclusion chromatography and additional lines of evidence suggest that moss PYLs are predominantly monomeric. A combination of mutational analysis with biochemical and physiological assays reveals that the reduced basal activities of moss PYLs are achieved through unique sets of amino acid variations. Finally, introducing the causal variations to dimeric receptors dramatically compromises their ABA-responsiveness, suggesting the two evolutionary trajectories are mutually exclusive. Hence, mosses appear to have evolved a parallel mechanism to mitigate the ancestrally high background signal of the core ABA perception apparatus. This convergence highlights the shared imperative of expanding the amplitude of a central, highly adaptive signaling pathway.

**Keywords:** PYR/PYL/RCAR | moss | abscisic acid | receptor basal activity | convergent evolution

# Introduction

Across the spectrum of life, organisms employ small organic molecules for intra- and intercellular communication. The levels and spatial distribution of small molecule-hormones respond to various stimuli *via* dedicated pathways, and their physiological effects are mediated by specialized signaling cascades controlling downstream transcriptional and metabolic networks. The functionality of these signaling molecules, therefore, relies on large arrays of genetic factors. This raises the question of how new signaling molecules emerge through natural selection. The association of a metabolic product with a protein possessing pre-existing or potential regulatory activity plays a central role in driving this process. Once this link is formed, secondary input and output factors can be further modulated, elaborated and fine-tuned in a manner that is highly specific for cell type, tissue and species. This, in turn, may facilitate a diversity of niche- and lifestyle-specific adaptations <sup>1</sup>.

The phytohormone Abscisic acid (ABA) is emerging as a seminal exemplar in the evolution of highly consequential signaling systems <sup>2</sup>. The functionality of this small organic molecule underpins an adaptation that was pivotal in altering terrestrial landscapes and shaping the trajectory of species development on our planet – namely, desiccation tolerance in plants. The transition to terrestrial habitats approximately 500 million years ago required the ability of pioneering plants to endure generally dry conditions while effectively managing cycles of dehydration and rewetting <sup>3</sup>. Distinct taxa within the terrestrial green lineage exhibit notable diversity in terms of their life cycles, morphological attributes, and mechanisms for coping with dehydration stress. Despite these variations, the involvement of ABA in facilitating desiccation survival appears as a unifying feature across distant clades of land plants <sup>4</sup>.

ABA-dependent dehydration responses were extensively described in angiosperms (flowering plants), the most dominant land plant clade. These responses include, for example, the reduction of water loss *via* stomatal closure <sup>5</sup>, the induced accumulation of protective compounds <sup>6</sup> and the promotion of seed dormancy and dehydration <sup>7</sup>. Analogous roles of ABA have been reported in gymnosperms <sup>8,9</sup> while for seedless vascular plants – ferns and lycophytes – evidence is sparse and the notion of ABA as a central mediator of dehydration responses is very much debatable <sup>10</sup>. Even so, despite diverging earlier from angiosperms, some non-vascular plants (bryophytes) do employ ABA to regulate key aspects of their adaptation to terrestrial habitats <sup>11</sup>. First, ABA signaling promotes successful recovery from near-complete dehydration (*i.e.* vegetative desiccation tolerance) by inducing the accumulation of protective LEA transcripts and metabolites in both mosses and liverworts <sup>12</sup>. Another way by which bryophytes persist through recurring cycles of prolonged dehydration is the formation of hardy, metabolically dormant

propagative units. In liverworts, ABA positively regulates the dormancy of asexual propagules<sup>13</sup>, while in mosses, it attenuates the germination of spores and promotes the differentiation of filamentous protonemata into specialized brood cells<sup>14,15</sup>.

The conserved significance of ABA is reflected in the widespread expression of a functional ABA signaling apparatus across all major lineages of land plants<sup>16</sup>. The first step in this canonical pathway involves a family of soluble receptors called PYRABACTIN RESISTANCE1/PYR1-LIKE/REGULATORY COMPONENT OF ABA RECEPTOR (PYR/PYL/RCAR)<sup>17,18</sup>. Upon ABA binding, these receptors (“PYLs”) form stable complexes with their co-receptor PP2C phosphatases, thereby inhibiting their enzymatic function and releasing a downstream phosphorylation cascade<sup>19</sup>. Notably, PYLs display a great deal of variation in several biochemical parameters that affect their signaling function<sup>20,21</sup>. For example, the inherent PP2C-inhibiting capacity – both basal (ligand-free) and at saturating ABA levels – varies substantially between different PYLs. Additionally, PYLs may differ in their intrinsic affinity for ABA. Their activities may therefore be dynamic (*i.e.* dose-responsive) along different ranges of ABA concentration – from sensitivity threshold to saturation. Hence, the overall ABA responsiveness of a given plant cell depends on the specific ensemble of PYLs it expresses.

In a previous study, taking a receptor-centric approach helped us to gain insight into the emergence of ABA’s hormonal function, tracing it back to the very origin of terrestrial plants. All land plants are considered to have descended from a single successful colonization event by a species of streptophyte alga<sup>22,23</sup>. ABA is widely present in this group of algae, but with few exceptions, does not seem to carry any significant physiological or cellular effects<sup>2</sup>. While aeroterrestrial streptophyte algae harbor most of the core genetic components that typify the ABA response of land plants, homologs of PYL receptors are found exclusively in the Zygnematophyceae<sup>24,25</sup> – sister group to all the land plants<sup>23</sup>. Recently, we showed that these algal PYL homologues do not bind ABA but exert substantial inhibition of PP2C phosphatases in an ABA-independent manner<sup>26</sup>. Hence, the signaling activity of PYLs likely coincided with the presence of ABA in a common ancestor of all land plants; ABA-mediated signaling arose through subsequent mutations in PYLs, which made them subject to chemical regulation by this preexisting metabolite. Consequently, the basal PP2C-inhibition capacity of ancestral PYLs likely represented an initial constraint on the utility of ABA in regulating responses to fluctuating environmental conditions.

The majority of PYLs expressed by extant plant species are still characterized by moderate to high levels of basal activity<sup>26</sup>. In this regard, members of the angiosperm-specific subfamily III are unique, as they display self-dimerization that ensures a relatively high level of ABA dependency for PP2C interaction<sup>27</sup>. Here, we

show that PYL receptors in the mosses comprise a phylogenetically divergent clade. Within the Bryophytina sub-division, PYLs have radiated further to form three subfamilies, whose members feature a relatively high ABA dependency despite being predominantly monomeric in solution. A series of genetic manipulations and biochemical assays point to specific divergent amino acids in otherwise conserved gate-loop and PP2C-interacting domains that underpin this gained functionality. Moreover, introducing this causal gate-variation into dimeric receptors results in a dramatically diminished ABA affinity, suggesting a degree of mutual exclusivity between the two evolutionary routes. Thus, Bryophytina mosses appear to have evolved a parallel molecular switch mechanism that increases ligand dependency for the core ABA signaling cascade.

## Results

### **Independent radiation of PYL receptors gave rise to ABA perception in mosses**

We opted to use PYL receptors as a vantage point to study the evolution of ABA signaling. The rationale for this strategy was that ABA, in and of itself, is an inert molecule and that mutations causing ancestral PYLs to shift towards ABA-induced activity were pivotal in the establishment of its signaling function. The last point is underscored by the complete ABA non-responsive (ANR) phenotype displayed by mutant lines of the moss *Physcomitrium patens* (previously *Physcomitrella*) in which all functional ABA-receptor genes were knocked out *via* CRISPR (Figures 1A-C and S1). Three independent lines were isolated based on observable ANR phenotypes (Figure 1A) and genetically characterized (Table S1). Disruptions in four genes – *PpPYLs 1-4* – were common to all three lines. Only one line was disrupted in *PpPYL5*, which was later shown to be a likely misclassified pseudogene. All three lines exhibited non-restricted growth in the presence of saturating levels of ABA in subsequent experiments (Figure 1B). Finally, each of the four individual native receptors rescued ABA-induced transcription in *Pppy1-4*-derived protoplasts, validating that the described genetic disruptions and the observed ANR phenotype are causally linked (Figure 1C). These results also indicate that between them, *PpPYLs 1-4* encompass the entire ABA response capacity of *P. patens*.

To study the early establishment of ABA mediated signaling, we performed a phylogenetic analysis using 536 PYL protein sequences from diverse plant lineages, with a particular focus on moss and angiosperm sequences for contextualization (Figure 1D). Our phylogenetic analysis loosely recovered the classification of the three canonical receptor subfamilies for – and based on – angiosperms<sup>17,18</sup>. In the genomes of two hornworts – *Anthoceros agrestis* and *A. punctatus*, we could detect only a single receptor that showed phylogenetic similarity to Angiosperm subfamily I. Subfamily I was also affiliated with a subgroup of receptors from early vascular plants (*i.e.* ferns and lycophytes), which is in line with our previous

phylogenetic analysis<sup>26</sup>. In contrast to hornwort PYLs, the Setaphyta (liverworts and mosses) receptors have a considerable sequence diversity. Interestingly, PYLs from moss species (Bryophytina and peat moss) do not cluster with the rest of the plant PYL subfamilies. Within the Bryophytina subdivision, several independent rounds of radiation gave rise to class- or order-specific clades (Bryopsida I to III), and all species investigated here (n = 37) encode two or more PYLs (Table S2). This clade-specific increase in the numbers and diversity of PYLs seems consistent with the well-documented adaptive role of ABA signaling in mosses<sup>14,15</sup>. However, the inferred phylogenetic structure also resembles the overall known relationships between bryophyte taxa (Figure 1E). Therefore, the possibility of it being driven by differential histories of whole-genome duplications and subsequent drift, still needs to be considered. We reason that if the newly observed expansion of moss PYLs is truly the result of some gained adaptive functionality, it would be reflected in their functionality at the basic biochemical level.

#### **ABA receptors from all Bryophytina-specific subfamilies display a high degree of ABA-dependency despite being monomeric**

In our previous study, we observed that basal activity generally reflects an ancestral feature of ABA receptors – likely a consequence of their ligand-independent origin<sup>26</sup>. Background signals exerted by basally active receptors might have a physiological role, but theoretically, it is also expected to constrain a hormone's ability to regulate proportional responses to dynamic stimuli. Hereafter, we use the term 'basal activity' specifically to describe the proportion of phosphatase inhibition exerted by ligand-free receptors out of their full PP2C inhibition capacity at ABA saturation. This definition is useful for addressing the very functionality of a given PYL, as it expresses its potential to be dynamically regulated by ABA, while absolute high or low values are, in and of themselves, adjustable through expression intensity. Next, we sought to complement the phylogenetic analysis by rigorously characterizing the basal vs ligand-induced activities of different bryophyte receptors. A panel of representative receptors was tested by yeast 2-hybrid (Y2H) and by measuring their activity *in vitro*. The latter assay was designed specifically to characterize each receptor's PP2C inhibition capacity in ligand-free vs. ABA-saturated states. All of the basal activity scores presented hereafter are calculated from reactions containing a PP2C:PYL molar ratio of 1:2 and comparisons are made only between reactions that use the same phosphatase preparation. The panel included a *Marchantia polymorpha* receptor alongside receptors from four additional liverwort species (*Marchantia paleacea*, *Lunularia cruciata*, *Riccia berychiana* and *Conocephalum conicum*), one from *Anthoceros agrestis* (hornwort), as well as a selection of receptors encompassing the three moss-specific subfamilies from three species of moss (*Physcomitrium patens*, *Tetraphis pellucida* and *Philonotis fontana*). All receptors from

hornworts and liverworts displayed a detectable ABA-independent interaction with the *Arabidopsis thaliana* PP2C HAB1 in Y2H and inhibited its phosphatase activity in a molar ratio-dependent manner (Figures 2A and S2A). Ligand-free inhibition of HAB1 by hornwort and liverwort PYLs ranged from ~30% to 60% of their activity at ABA saturation (Figure 2B). By contrast, moss receptors generally displayed only negligible basal activities. They had no detectable ABA-independent interaction with HAB1 in Y2H and with the exception of PpPYL1, did not exert a molar ratio-dependent inhibition of HAB1 in the absence of ABA (Figures 2A-B and S2A). These results were also obtained when representative PYLs from mosses and liverworts were tested with their native PP2C co-receptors (Figure S2B). Hence, based on two independent biochemical assays, mosses seem to have diverged from hornworts and liverworts, encoding PYLs with reduced basal activity. The small number of PYLs found in hornwort and liverwort genomes and the high basal activities they display serve as further evidence for the last common ancestor of all terrestrial plants harboring a small number of receptors, whose activities are mostly ABA-independent.

In the case of angiosperm subfamily III receptors, the stricter requirement for ABA is a consequence of their tendency to form dimers in their open-gate *apo* state<sup>27</sup>. The dimers are configured in a manner that masks their PP2C-interface, thereby reducing the rate of transient PP2C interactions. Given the similar high ligand dependency displayed by moss PYLs, we naturally suspected a similar mechanism might be at work. To test this, we performed size-exclusion chromatography (SEC) on a set of representative receptors: AaPYL1 – hornwort, MpPYL1 – liverwort, PfPYL4 – Bryopsida I and TpPYL1 – Bryopsida II. For comparison, the analysis also included PYL1 and PYL10 from *Arabidopsis thaliana*, which are well established as dimeric and monomeric receptors, respectively<sup>28</sup>. All of these PYLs, with the single exception of AtPYL1, yielded SEC chromatograms that are consistent with a favorably monomeric state (Figure 2C). While assuring a high degree of ligand dependency, the dimerization of angiosperm subfamily III receptors also carries a penalty on their intrinsic affinity for ABA, as the requirement for dimer-dissociation thermodynamically disfavors ABA-binding<sup>27</sup>. Consequently, Angiosperm subfamily III receptors typically display K<sub>d</sub> values ranging from 50 to 100 μM. Two Bryopsida II (PpPYL1, TpPYL1) and one Bryopsida I (PfPYL4) receptors tested here by isothermal titration calorimetry (ITC) displayed K<sub>d</sub> values in the typical range of monomeric PYLs, with at least 10-times lower K<sub>d</sub> than the Angiosperm subfamily III receptors (Figures S3). Hence, the low background activity of moss receptors from at least two subfamilies (I and II) appears to be an intrinsic property of their ligand-free state, rather than a consequence of their oligomeric status.

### Single Gate-Loop Residue Dictates ABA Dependency in Bryopsida Subfamilies II and III

Next, we sought to pinpoint the specific sequence variations that are responsible for the higher ABA dependence of moss receptors. We generated a dataset of 13 functionally characterized receptors (*Arabidopsis thaliana*, *Selaginella moellendorffii*, *Anthoceros agrestis*, *Marchantia polymorpha*, *Lunularia cruciata*, *Tetraphis pellucida*, *Philonotis fontana* and *Physcomitrium patens*). Criteria for outlying residues were either high conservation, specifically within moss receptors, or divergent residues that are conserved across all non-moss plants. Six positions met these criteria, all of which reside in regions that are known to be involved in PP2C binding and their flanking sequence (Figure S4). Consensus logos of these regions were generated from 134 Bryophytina ABA receptors and 315 receptors from plants in other phyla (Figure 2D). Four regions containing anomalies in the smaller receptor dataset were consistent with the results of the wider comparison when evaluating the entire database. The regions include the gate and latch sequences, the C-terminal helix sequence, and the adjacent loops. The gate sequence motif (SGLPA) is highly conserved across all non-moss plant phyla. By contrast, the gate in Bryophytina is not nearly as consistent, containing variation in the second and third residues of the gate (Figure 2D). Despite being somewhat conservative in their corresponding chemical properties, we suspected these two moss-specific variations to be functionally consequential. It is also noteworthy that among all 134 Bryophytina receptors, only three types of gate variations are represented and they segregate tightly between the three phylogenetically predefined subfamilies (Bryopsida I = **S**GI**P**A, Bryopsida II = **S**SI**P**A, Bryopsida III = **S**S**V****P**A). The residue immediately following the latch sequence, which is predominantly Glutamine (uncharged polar) in mosses, while positively charged in all other plants (Figures 2D and S4A), was also subjected to further inspection, as well as three additional divergent residues located at, or adjacent to PP2C binding regions (corresponding to T57, H60, and R157 in AtPYR1 coordinates).

We generated two sets of mutants at the six suspected causal residues and also a double mutant changing both gate residues simultaneously. In the first set, these positions in MpPYL1 from the liverwort *M. polymorpha* were substituted by the corresponding amino acids present in Bryophytina II PYLs. The second set contained all reciprocal substitutions in the background PpPYL1 from the moss *P. patens*. Our aim was to identify a variation that is sufficient both to raise the basal activity of a *P. patens* receptor and, conversely, to lower the basal activity of the *M. polymorpha* receptor MpPYL1. Identifying a residue carrying this type of effect would potentially suffice to explain the ABA-dependent nature of moss receptors from subfamilies II and III. Each variant receptor was tested by Y2H and *in*

*in vitro* by a phosphatase inhibition assay against HAB1 (Figure 3) and against its native phosphatase – PpABI1A or MpABI1 from *P. patens* and *M. polymorpha*, respectively (Figure S5). This screen showed that mutating the second gate position (Ser to Gly and *vice versa*) is sufficient to elicit this type of bidirectional effect, increasing the basal activity of PpPYL1 from 6% to 41% (Figures 3A and S5A) and reducing that of MpPYL1 from 40% to 1.5% (Figures 3B and S5B). The third gate position alone had a marginal effect on the basal activity of PpPYL1. However, when tested against its native PP2C – PpABI1A, it had a synergistic effect with the second gate position, further increasing PpPYL1 basal activity from 41% to 70% (Figure S5A). Introducing the MpPYL1-type gate variation (SGLPA) also increased the basal activity of two additional moss receptors from Bryopsida subfamilies II and III (Figures S6A-B). None of these mutations had any negative effect on the activity of either receptor at a saturating ABA concentration. Thus, the reduced basal activity of receptors from Bryopsida subfamilies II and III is almost fully explained by a single glycine to serine substitution at a highly conserved gate-loop position.

We have performed a complementary experiment to test if the observed basal activities (or lack thereof) are sufficient to alter the degree to which bryophyte PYLs induce measurable ABA responses *in planta*. PYLs that are characterized by high basal activity can rescue various ABA-deficiency phenotypes partly owing to constitutive activation of the ABA downstream signaling cascade<sup>26</sup>. The ABA-deficient Arabidopsis mutant *aba2-1* displays a reduced stature and an elevated baseline transpiration rate, which can be measured indirectly through thermal imaging. This mutant was transformed with the wild type, or gate-mutated variants of MpPYL1, PpPYL1, and PpPYL3, under the promoter of AtPYL4 (Figures 4 and S6C-D). Receptor variants, biochemically characterized here as having high basal activity (MpPYL1 - wild type; PpPYL1 - S89G/I90L; PpPYL3 – S90G/V91L), significantly increased both fresh weight and leaf temperature relative to the ABA-deficient genetic background, with PpPYL1 - S89G/I90L being statistically indistinguishable from the non-ABA deficient wild type Arabidopsis. In contrast, variants that displayed low basal activity in the biochemical assays (MpPYL1 – G83S/L84I; PpPYL1 – wild type; PpPYL3 – wild type) did not significantly affect either of the two ABA-deficiency phenotypes. Hence, the reduced basal activity conferred by the glycine to serine substitution prevents moss receptors from exerting the same degree of constitutive signal elicited by a liverwort PYL *in planta*. Moreover, these results reaffirm the ability of basal activity to generate an elevated background signal, thereby limiting the dynamic nature of ABA-regulated processes. The potential physiological impact is further evident from the activation of ABA signaling in *P. patens*

*Pppyl1-4* protoplasts expressing ZcPYL8– an algal PYL homolog that cannot bind ABA but exhibits ligand-independent activity comparable to that of liverwort and hornwort PYLs in the absence of ABA<sup>26</sup> (Figure S1B).

### **The basal activity-reducing gate-variation carries a subfamily dependent side-effect**

A network of dehydration stress responses was brought under the regulation of ABA-triggered PYL-PP2C interaction in a common ancestor of land plants<sup>29</sup>. While increasing survivability under water deficit, stress-coping programs are by nature costly in terms of resource allocation. For example, the growth-inhibiting effect of activated ABA signaling, as seen in Figure 1A-B and reported previously<sup>13,30</sup>. Maximizing overall fitness in light of these tradeoffs would favor ABA-regulated responses that are quantitatively proportional to experienced stress or to “perceived” risk thereof<sup>31</sup>. The Glycine to Serine substitution described here above appears to be a readily available evolutionary route to achieve this, potentially requiring only a single base substitution to increase the amplitude of downstream signal intensity in an ABA dose-dependent manner. However, this specific gate variation is restricted to two Bryophytina-specific subfamilies (II and III). Its absence in other plant taxa could be explained by a possible negative effect on other aspects of the receptor’s function, which is mitigated by the epistatic action of other co-mutated residues.

To evaluate this possibility, we introduced Serine to the second gate-loop position in a series of receptors, representing different subfamilies from angiosperms and bryophytes. Wild-type and gate-mutated variants were tested both for ABA-dose-responsive PP2C inhibition (Figure 5) and for their intrinsic binding affinity for ABA by ITC (Figure S3). The gate mutated version of the liverwort receptor MpPYL1 displayed both a diminished ABA dose-response curve (4-fold increase in IC<sub>50</sub>) and a 3-fold reduction in ABA binding affinity, relative to the wild type (Figures 5A and 3A). The Bryopsida I receptor PfpYL4 was similarly affected, with its activity’s IC<sub>50</sub> and dissociation constant increasing 10-fold and 4-fold, respectively (Figures 5B and S3B). Affecting not only the receptor’s affinity for ABA but also its ABA-triggered activity stands as another contrast to the pattern observed with dimeric receptors, where the disfavored thermodynamics of dimer dissociation is balanced out by the stability of the ternary (PYL-ABA-PP2C) complex<sup>27</sup>. Reversing the second gate-loop position of a Bryopsida II receptor from Serine back to Glycine did not substantially change its K<sub>d</sub>, nor did it result in reduced sensitivity to ABA in the PP2C-inhibition assay (Figures 5C and S3C).

In angiosperms, the consequence of substituting the second gate position from Glycine to Serine was subfamily-dependent. The basal activity of two Arabidopsis Subfamily II receptors AtPYL5 and AtPYL6 (22% and 28%, respectively) was effectively nullified when they were introduced with the moss-type gate variation (Figure S7), and their ABA dose-response curve was not substantially affected (Figure 5E). Subfamily I members, on the other hand, displayed no apparent reduction in basal activity (Figure S7) and were compromised in their ABA-triggered activity, with a 5-fold increase in the IC50 values of AtPYL8 and AtPYL10 (Figure 5D). For subfamily III dimeric receptors, the negative effect was especially dramatic, with IC50 values of PP2C inhibition increasing by 2 orders of magnitude (Figure 5F). The binding affinity of ABA for the gate-mutated PYL2 from Arabidopsis was substantially weakened relative to the wild type ( $K_d=56 \mu\text{M}$ ) and its  $K_d$  could not be determined by ITC (Figure S3E). Overall, these results confirm that when introduced alone, the Bryopsida II/III-type gate variation carries a potentially negative effect. This trade-off is subfamily-dependent, indicating that additional mutations are required to render the gate-variation adaptive and explaining its absence from several other PYL subfamilies. The functional loss observed in dimeric receptors indicates that the basal activity-reducing mechanism of certain Bryopsida receptors is not only distinct from that of angiosperm subfamily III receptors but also that the two mechanisms—or their respective genetic determinants—are mutually exclusive.

#### **Bryopsida subfamily I receptors assume high ligand dependency through the dispersed effect of several amino acid variations**

The straightforward and dominant effect of the Bryopsida II/III-type gate variation does not explain the ligand-dependent activity of Bryopsida I receptors, which feature a near-canonical (SGIPA) gate. Out of the remaining variations that were originally inspected, two substitutions - K115Q and M154H in MpPYL1 coordinates – are unique to mosses and highly conserved across all three Bryopsida subfamilies. The latter position, located adjacent to a C-terminal helix, is variant only among PYLs from peat mosses – a divergent group outside the Bryophytina<sup>32</sup>. Therefore, both variations likely existed in a single receptor gene within the common ancestor of all true mosses, which subsequently radiated and gave rise to all members of the three designated Bryopsida PYL subfamilies. The K115Q substitution had no observable effect on ABA-independent PP2C interaction in Y2H, but it partially reduced the basal activity of MpPYL1 (Figures 3B and S5B). The reciprocal mutant – Q126K in PfPYL4 (Bryopsida I) – had no effect in either of the assays (Figure 6A). In contrast, the two reciprocal mutations – MpPYL1 M154H and PfPYL4 H165M – did carry opposite effects on the basal activities of their

respective backgrounds. However, they only marginally affected *in vivo* PP2C interaction, and contrary to the Bryopsida II/III-type variation, their effect in PP2C inhibition was partial – not explaining the full difference in basal activity between liverwort and Bryopsida I receptors (Figures 3B and 6).

We used a revised set of criteria to find sequence variations that might explain the increased ABA-dependence of Bryopsida I receptors. Five positions that are conserved between liverwort and Bryopsida II/III receptors but divergent and conserved within Bryopsida I were selected (positions R79, F105, S133, M146, and R173 in MpPYL1 coordinates). All positions were mutated in MpPYL1 to their respective residues as present in PfpYL4 and vice versa. The resulting PfpYL4 and MpPYL1 variants were tested by Y2H against the moss and liverwort PP2Cs PpABI1A and MpABI1, respectively. No single mutation had a notable effect on Y2H LacZ staining in the absence of ABA, whereas positive staining for PYL-PP2C interaction under 10  $\mu$ M ABA was unaffected. Next, we engaged in higher-order reciprocal mutagenesis between MpPYL1 and PfpYL4 to obtain a bidirectional combinatorial panel. We also included the PfpYL4 M154H and MpPYL1 H165M substitution, as it had a partial effect and likely predated the divergence of subfamily I, making it the relevant background within which all other mutations took place. The reciprocal panel included all five mutations in the background of the M154H/H165M substitution. Two variants harboring all six substitutions were also created to test if together they account for the difference in ABA-independent PP2C interaction between the two representative PYLs. We also wanted to evaluate if any of the substitutions are indispensable for this difference. For this specific purpose, we also created all six quintuple mutants, where one mutation is excluded, as well as five quadruple mutants, in which M154H/H165M plus one of the other mutations are omitted.

The reciprocal panel was first screened by Y2H. All mutants in both backgrounds displayed normal interaction with their respective phosphatases in the presence of 10  $\mu$ M ABA, evident by strong LacZ staining intensity. The PfpYL4 sextuple mutant displayed strong ABA-independent interaction with PpABI1A (Figure 6B), and the basal interaction between MpPYL1 and MpABI1 was reduced below visible levels when all six mutations were introduced (Figure S8). All quintuple mutants in the PfpYL4 background also displayed a detectable basal PP2C interaction. However, the exclusion of F90R, W116F, or H165M resulted in a slightly reduced staining intensity (Figure 6B). A single PfpYL4 double mutant (F90R; H165M) displayed ABA-independent interaction with PpABI1A, suggesting a dominant role for these two residues. While no MpPYL1 single or double mutant exhibited any visible difference from

the wild type protein, basal MpABI1 affinity was reduced in all higher-order mutants. The added effect of the five mutations, observed here by Y2H, did not translate to an *in vitro* PP2C inhibition-type assay in any straightforward manner. The basal activity observed for several quintuple and quadruple mutants did not substantially differ from that of the H165M single mutant. However, it is notable that the quintuple PpPYL4 mutant, in which H165M is excluded, did not inhibit PpABI1A activity in the absence of ABA, while its ABA-triggered inhibition was unaffected. Also, the single mutant F90R displayed a degree of basal activity that is comparable with that of PpPYL4 H165M.

Overall, the screen failed to identify any simple, straightforward logic that fully explains the loss of basal activity in Bryopsida subfamily I receptors. It is conceivable that such logic exists, but it was missed. Nevertheless, it seems that compared with the case of subfamilies II and III, the transition to high ligand-dependency in the Bryopsida subfamily I was facilitated owing to the rather dispersed, cumulative effect of several substitutions. Therefore, Bryopsida subfamily I converged with subfamilies II and III towards reduced basal PP2C inhibition *via* a distinct set of genetic determinants.

## Discussion

Mosses and angiosperms both utilize ABA signaling to regulate equivalent sets of responses to water scarcity that are key adaptations to their terrestrial lifestyle. According to the principle of biological optimality, networks of ABA-regulated processes are shaped by natural selection, not only to promote survivability under fluctuating conditions but also to integrate conflicting considerations such as growth, reproduction, and competitiveness<sup>31</sup>. Doing so requires the ability to mount quantitatively proportional responses in a conditional manner. The cumulative body of evidence indicates that the last common ancestor of all embryophytes, which existed *circa* 500 million years ago, likely possessed a small number of PYLs – potentially even a single gene – that featured a high degree of basal activity. Given the demonstrated ability of high-basal-activity PYLs to activate ABA responses independently of ABA and in physiological contexts (as shown here in Figures 4, S1B, and S6C-D, and in previous studies<sup>26,33</sup>), it is plausible that the narrow dynamic range of these ancestral PYLs constrained the capacity of ABA to elicit quantitatively tuned responses. Moreover, the evolution of elaborately conditional ABA responses (*e.g.* tissue-specific or modulated by current or previously experienced external conditions) was likely limited by the low number of PYL genes.

In angiosperms, the prominence of ABA is reflected in the expansion of its receptors, which diversified to form three subfamilies whose members exhibit a certain degree of specialization in their functionalities and expression patterns<sup>34</sup>. Here, our phylogenetic analysis showed that the expansion that gave rise to all moss PYLs was lineage-specific, thus wholly independent from the diversification of PYLs in all other embryophyte phyla. Given our findings regarding hornwort as well as liverwort species, it seems that the common ancestor of all bryophytes still featured a low number of abscisic acid receptors, exhibiting high basal activity. The radiation of Bryophytina PYLs and their reduced ABA-independent activities, are both consistent with the well documented adaptive roles of ABA in this clade of land plants. Like mosses, liverworts are also known to utilize ABA to regulate dehydration responses. It remains an open question whether liverworts somehow fundamentally differ from mosses in the nature of their ABA-dependent processes or whether they employ an alternative mechanism to achieve a similar degree of responsiveness using a less diversified, less dynamic ABA signal transduction apparatus.

Our biochemical experiments indicate that the strict ligand-dependency of multiple Bryopsida PYLs is not achieved through self-dimerization; hence, it is most likely an intrinsic property of their *apo* state.

Previous studies have shown that ligand-free PYLs exist in a two-state conformational equilibrium, which can be shifted by certain mutations to favor (or disfavor) PP2C-interaction<sup>33</sup>. Alternatively, the specific mutations might act by destabilizing PYL-PP2C complexes in the absence of ABA. While the specific underlying mechanism remains to be elucidated, it is evidently distinct from that of angiosperm subfamily III PYLs, and involves different genetic determinants. Features that evolve multiple times independently across different taxa generally hint at a common adaptive imperative. Here, we have demonstrated that abscisic acid receptors display functional convergence towards reduced background activity between two distant clades of land plants and also between different subfamilies within the Bryophytina. This specific case of convergent evolution underscores the reduction of basal signaling by receptors (or, more generally, the expansion of their dynamic range) as an additional key trend in the evolution of hormonal regulation.

# STAR methods

## EXPERIMENTAL MODEL AND STUDY PARTICIPANT DETAILS

### *Plant material and growth conditions.*

The ‘Gransden’ strain of *Physcomitrium patens* (Hedw.) was used as background for the generation of described mutants. Protonemal culture was maintained as described previously<sup>35</sup> and vegetatively propagated by homogenization and subculture every 7 days.

All Arabidopsis lines used in experiments were in the Columbia (Col-0) background. The *aba2-1* mutant<sup>36</sup> was used for ABA-deficiency suppression assays. *A. thaliana* plants were grown in a growth chamber (Percival Scientific USA) under controlled light-intensity (70 to 100  $\mu\text{E}\cdot\text{m}^{-2}\cdot\text{s}^{-1}$ ) and temperature (20-22 °C) conditions. A long day diurnal period (16 h light/ 8 h dark) light period was used for plant propagation and a short-day period (10 h light/ 14 h dark) was used for ABA-deficient phenotype-suppression assays.

### Key resources table

REAGENT or RESOURCE	SOURCE	IDENTIFIER
Bacterial and virus strains		
E. Coli strain DH5 $\alpha$		
E. coli strain BL21 (DE3) ) <i>pLysS</i>	Promega	CAT# L1195
Chemicals, peptides, and recombinant proteins		
(+)-Abscisic acid		CAS No 21293-29-8
G418 disulfate	TOKU-E	CAT# G001 / CAS 108321-42-2
IPTG		CAS No 367-93-1
pNPP	Sigma Aldrich	CAT# 487663 / CAS 36199-67-4
Imidasole	Sigma Aldrich	CAS No 288-32-4
$\beta$ -Me	Sigma Aldrich	CAS No 60-24-2
DTT	Sigma Aldrich	CAS No 3483-12-3
Glufosinate-ammonium	Sigma Aldrich	CAT# 45520 / CAS 77182-82-2
Methylumbelliferyl glucuronide		CAS No 6160-80-1
Luminol		CAS No 521-31-3
Critical commercial assays		
Ni-NTA agarose	Cube biotech	31105
Gel filtration calibration kit LMW	Cytiva	28403841
QuikChange Lightning Multi Site-Directed Mutagenesis	Agilent	210515

Deposited data		
<i>P. patens</i> genome browser	Perroud <i>et al.</i> <sup>37</sup>	
Experimental models: Organisms/strains		
Physcomitrium patens (Gransden strain)		
Physcomitrium patens (Gransden strain) <i>Pppy1-4</i>	This paper	
saccharomyces cerevisiae strain Y190 ( <i>MAT<math>\alpha</math></i> , <i>ade2-101</i> , <i>gal4</i> , <i>gal80</i> , <i>his3 -200</i> , <i>leu2-3,112</i> <i>trp1 -901</i> , <i>ura3-52</i> , <i>URA3::GAL1-lacZ</i> , <i>lys2::GAL1-HIS3</i> , <i>cyhrs</i> )		
<i>Arabidopsis thaliana</i> (ecotype Col-0)		
<i>aba2-1</i> (Col-0 background)	Léon-Kloosterziel <i>et al.</i> <sup>36</sup>	
Recombinant DNA		
pEn-Chimera	Addgene	ID 61432
pMBL::Ubi-Cas-nos	This paper	
pHeGHPB	Pri-Tal <i>et al.</i> <sup>34</sup>	
pMBL5::YFP	This paper	
pBM113Kp	Knight <i>et al.</i> <sup>38</sup>	
pAct1-LUC	Mcelroy <i>et al.</i> <sup>39</sup>	
pBD-GAL4 Cam	Clontech	
pACT2	Clontech	
pET28	Novagen	CAT# 69864-3
Software and algorithms		
MAFFT (v.7.305b)	Katoh <i>et al.</i> <sup>40</sup>	
IQ-TREE multicore version 1.5.5	Nguyen <i>et al.</i> <sup>41</sup>	
Modelfinder	Kalyaanamoorthy <i>et al.</i> <sup>42</sup>	
CRISPOR	Concordet <i>et al.</i> <sup>43</sup>	
FLIR Tools v5.2.15161.1001 software	FLIR	
JMP pro 12 statistical package	SAS Institute	
Other		
Epoch Microplate Spectrophotometer	BioTek	
MicroCal iTC200 system	Malvern Panalytical	
Superdex 75 10/300 GL	Cytiva	
FLIR T630 camera	FLIR	
Fluostar Optima	BMG LABTECH	

## METHOD DETAILS

**DNA Sequence.** Coding sequences of all bryophyte PYLs,  $\Delta$ N PpABI1A (lacking N-terminal amino acids

1 to 105),  $\Delta$ N MpABI1 (lacking residues 1 to 224 were obtained via chemical synthesis (Table S3) or from a previous study. The AtPYL4 promoter (1425 bp upstream from the start codon), was amplified from Col-0 genomic DNA. *Arabidopsis thaliana* PYLs were amplified by PCR, using a template of Col-0 genomic DNA, or seedling-extracted cDNA for intron-containing genes. All PCR amplifications were carried out using a Phusion High-Fidelity DNA Polymerase (New England Biolabs).

**Phylogenetic analyses of PYL sequences.** PYL homologs were sampled across all major phyla of embryophytes from 1KP database (<https://db.cngb.org/onekp/>) by performing BLAST, with a focus on the mosses. 536 PYL protein sequences were aligned using MAFFT (v.7.305b) and a strategy using local pairwise alignment information (L-INS-I)<sup>40</sup>. IQ-TREE multicore version 1.5.5 for Linux 64-bit<sup>41</sup> was used to compute a maximum likelihood phylogeny, using the best model according to Bayesian Information Criterion (JTT+G4) determined by Modelfinder<sup>42</sup> 500 bootstrap pseudoreplicates were computed.

**CRISPR-Cas9 plasmid constructions.** Vectors for CRISPR-Cas9 mutagenesis were the single-guide RNA construct pEn-Chimera (Addgene ID 61432) and a Cas9-containing vector modified by reconstruction from pDE-Cas9 (Addgene ID 612433) in the *P. patens* specific vector pMBL5<sup>44,45</sup>. The PsUBi4-2 promoter and the Cas9-SSU-terminator coding fragments were recovered from pDE-Cas9 by *EcoRI* digestion. The Cas9-SSU terminator fragment was ligated into the *EcoRI* site of pMBL5, and digestion with *Ecl136II* deleted the terminator and 3'-terminal *EcoRI* site, allowing the Ubi promoter to be ligated into the remaining *EcoRI* site in pMBL5. Finally, a nopaline synthetase terminator fragment cloned as an *EcoRI/Ecl136II* fragment in pBluescript was recovered by digestion of this plasmid with *EcoRV* and *Ecl136II* for blunt-end ligation into the corresponding site in the pMBL-based plasmid to create the plasmid pMBL::Ubi-Cas-nos.

**Generation of and characterization *P. patens* pyl mutants.** PYL-deficient mutants of *Physcomitrella* (*Physcomitrium patens*) were generated using multiplex CRISPR-Cas9 mutagenesis following transient transfection of *P. patens* protoplasts<sup>46</sup>. Chloronemal tissue of *P. patens* (Gransden strain) was propagated on BCDAT agar medium overlain with cellophane discs for preparation of protoplasts and transformation with plasmid DNA as previously described<sup>35,45</sup>. For CRISPR-Cas9 mutagenesis, protoplasts were transfected with 22  $\mu$ g of plasmid DNA comprising an equimolar mixture of 6 circular plasmids: the pMBL-Ubi-Cas-nos expression construct (assembled in the *P. patens* transformation vector pMBL5 containing an NPTII selection cassette) and the other 5 – pPyg26; pPysg13; pPysg7; pPysg9; pPysg3 – each containing a single-guide RNA sequence targeting one of the five *P. patens* PYL homologues Pp3c26\_15240 (“PpPYL1”); Pp3c13\_7110 (“PpPYL2”); Pp3c7\_26290 (“PpPYL3”); Pp3c9\_19760 (“PpPYL4”); Pp3c3\_660 (“PpPYL5”) ligated into the two *BbsI* sites in the plasmid pEn-Chimera. Oligonucleotides for the construction of single-

guide sequences were identified using the CRISPOR software (<http://crispor.tefor.net>; <sup>43</sup>). Following transfection, protoplasts were allowed to regenerate overnight in PRM-L (liquid) medium before being embedded in PRM-T (top) agar medium (BCDAT containing 6% [w/v] mannitol, 10 mM CaCl<sub>2</sub>, and 0.4% agar) on cellophane overlaying the same medium containing 0.55% (w/v) agar in Petri dishes. Protoplasts were left to recover for 5-6 days without selection, until they were observed to be dividing. The cellophanes were then transferred to BCDAT medium containing 30mg l<sup>-1</sup> of the antibiotic G418 and 10<sup>-5</sup>M ABA, to select for transfected plants and to medium containing ABA (10<sup>-5</sup>M) for a further 10 days, to identify ABA non-responsive (ANR) mutants <sup>47</sup>. The majority of initial regenerants were rapidly killed by the antibiotic, and ABA non-responsive regenerants could be easily recognized by their unrestricted growth habit (Figure 1A).

We recovered in excess of 150 ANR plants following three independent transformations. An initial selection was made by inoculating plates with and without ABA supplementation at 10<sup>-5</sup>M with explants from this collection. Three of the most clearly ABA non-responsive lines (*Py7*, *Py15*, *Py24*) were then selected for production of protonemal homogenates for more detailed analysis. Growth tests of wild-type and mutant plants were carried out by measuring the increase in the size of explants regenerating on BCDAT agar medium in the presence and absence of ABA at 10<sup>-6</sup>, 10<sup>-5</sup> and 10<sup>-4</sup> M. The 'growth index' was calculated by image analysis of digital photographs taken at 3-day intervals between 4 and 19d following inoculation, using ImageJ as previously described <sup>48</sup>, with the pixel area of each explant normalized to the mean pixel area of 16 8 mm diameter black circles around the Petri dish. *PYL* transcripts were PCR-amplified from mutant cDNA or genomic DNA and sequenced. The *Pp3c3\_660* (*PpPYL5*) sequence could not be amplified from cDNA, and inspection of a number of RNAseq databases indicated that this locus was represented by none or only few reads in most individual transcript analyses. In the *P. patens* genome browser ([https://phytozome-next.jgi.doe.gov/info/Ppatens\\_v3\\_3](https://phytozome-next.jgi.doe.gov/info/Ppatens_v3_3); <sup>37</sup>) which provides comprehensive cumulative log-scale RNAseq coverage of all loci, overall transcript abundance for this locus is at least 2 orders of magnitude lower than for the other four *PYL* homologues. Consequently, the genomic sequence was amplified and sequenced for this locus. Candidate *pyl* mutants were selected and sub-cultured on BCDAT medium containing ABA but lacking antibiotic, in order to purge the plants of plasmids.

***Pppy1-4* Complementation assay.** Moss protoplasts derived from the *Pppy1-4* mutant line *Py15* (classified as *Pppy1-4* given the reevaluation of *PpPYL5*'s functionality – see Table S1) were used for genetic complementation analysis by transient expression of *PYL* genes. Full coding sequences of *PpPYLs* 1 to 4 from *P. patens*, as well as *ZcPYL8* from *Zygnema circumcarinatum* were cloned into

pMBL5::YFP, in which the coding sequences were fused in-frame with a YFP-coding sequence under the control of a 2x CaMV35S promoter. Protoplasts were isolated and transfected with a mixture of three plasmids: An ABA-reporter plasmid (pBM113Kp) containing the  $\beta$ -glucuronidase (GUS) gene under the control of the ABA-inducible wheat "Em" promoter<sup>4938</sup>; a reference plasmid, (pAct1-LUC) containing a firefly luciferase gene (LUC) driven by the rice actin-1 promoter<sup>39</sup>, and a "helper" plasmids carrying one of the five tested PYLs. Each of the transfected protoplast suspension was divided into aliquots and incubated for 24 hours with or without ABA (10  $\mu$ M). Protoplasts were subsequently recovered by centrifugation and lysed for the measurement of luciferase activity and  $\beta$ -glucuronidase activity. Beta-glucuronidase activity was determined by fluorometric measurement of the production of 5-methyl umbelliferone from methylumbelliferyl glucuronide<sup>50</sup>, while luciferase activity was determined by the luminescence intensity following injection of luminol. Activities were measured using the fluorescence and luminescence functions, respectively, of a Fluostar Optima instrument. Relative GUS activity was determined as GUS activity per 1000 luminescence units.

**Yeast Two-Hybrid.** The coding regions of receptors and PP2C phosphatases, were cloned into pBD-GAL4 and pACT2 (Clontech), respectively. Both pBD-GAL4 and pACT2 were co-transformed into *Saccharomyces cerevisiae* strain Y190, and positive colonies were selected on synthetic dextrose media, lacking *Leu* and *Trp*. Resulting strains were suspended and re-plated as dots on selective media containing either 10  $\mu$ M ABA or 0.1% DMSO as negative control. Plates were incubated at 30 °C for 2 d, and interaction was then tested based on  $\beta$ -galactosidase reporter-gene expression, using a chloroform-agarose overlay method<sup>18</sup>.

**Receptor-mediated PP2C inhibition assay.** The coding sequences of all bryophyte PYLs and  $\Delta$ N PpABI1A (lacking N-terminal amino acids 1 to 105) were cloned into the pET28 vector generating 6 $\times$ His-PYLs and 6 $\times$ His-PpABI1A. *Arabidopsis* PYLs,  $\Delta$ N HAB1,  $\Delta$ N MpABI1 were described previously<sup>26,51,52</sup>. Proteins were expressed in BL21 (DE3) pLysS (Promega) *E. coli* strain. For PYLs, transformed cells were pre-cultured overnight and then transferred into 500 mL terrific broth medium and cultured at 30 °C to OD600 = 0.9. IPTG was then added to a final concentration of 1 mM, and cultures were further incubated at 15 °C, overnight. For PP2C, MgCl<sub>2</sub> and IPTG were added to a final concentration of 1 mM each, at OD600 = 0.9. Samples were subsequently incubated overnight, at 18 °C. Cells were collected by centrifugation, suspended in buffer "A" (50 mM NaH<sub>2</sub>PO<sub>4</sub>, 300 mM NaCl at pH 8.0) plus 10 mM imidazole and stored at -80 °C. Lysis was performed by 2 freeze-thaw cycles followed by sonication for

60 s. Centrifugation was then performed, and cleared supernatant was loaded onto Ni-NTA agarose (Cube biotech), which was then washed with buffer A supplemented with 30 mM imidazole. Proteins were eluted with buffer "A" plus 250 mM imidazole. Recombinant proteins were dialyzed with 1 × TBS (50 mM Tris, 150 mM NaCl at pH 7.5), 20% glycerol, in 4 °C, overnight. For purification of PP2C, MgCl<sub>2</sub> (1 mM final concentration) was added to all buffers. A receptor-mediated PP2C inhibition assay was performed as previously described<sup>53</sup>. Reactions comprised 0.5 μM PP2C and 0, 0.5, 1, or 2 μM receptor and 33 mM Tris·acetate (pH 7.9), 66 mM potassium acetate, 0.1% BSA, 10 mM MnCl<sub>2</sub>, 0.1% β-ME, and 50 mM pNPP in the absence or presence of 10 μM ABA. Hydrolysis of pNPP was monitored at A405 by Epoch Microplate Spectrophotometer (BioTek). PP2C activity in the absence of receptor was set as 100% activity. The ABA dose-dependent PP2C inhibition assay was conducted as previously described<sup>52</sup>, using 0.5 μM PP2C, and 1 μM receptor. ABA was added at 0, 0.01, 0.025, 0.05, 0.1, 1, and 10 μM. PP2C activity in the presence of receptor and absence of ABA was set as 100% activity. All experiments were performed with 2 independent protein preparations.

**Isothermal titration calorimetry.** Proteins for isothermal titration calorimetry (ITC) were dialyzed with ITC buffer containing 20 mM Tris at pH 7.5, 150 mM NaCl, 1 mM β-mercaptoethanol. All PYLs were assayed at concentrations of 25 μM and temperature conditions of 25 C°. Protein solution in the cell was titrated with the ligand (+)ABA (400 μM) dissolved in the dialysis buffer. ITC experiments were executed in ITC200 by a series of injections of 3 μL ABA into the ITC cell containing PYL, and heat was measured after the injection. The calorimetric analysis program in the Origin suite was used for data evaluation and presentation.

**SEC analysis.** A solution of 0.6 μg/μl of each protein (AtPYL1, AtPYL10, TpPYL1, MpPYL1, AaPYL1 and PfPYL4) was loaded onto a 10/300 GL Superdex 75 increase column equilibrated and eluted with 50 mM Hepes pH 7.5, 150 mM NaCl, 5 mM MgCl<sub>2</sub> and 5 mM DTT buffer at a flow rate of 0.4 ml/min. The molecular marker profile was obtained from the SEC elution profile of a protein mix (gel filtration calibration kit LMW, Cytiva) at 0.6 μg/μl performed in similar conditions.

**Site-directed mutagenesis.** Mutations were introduced to pBD-GAL4 plasmids containing each respective receptor-gene using the QuikChange Lightning Multi Site-Directed Mutagenesis Kit (Agilent), according to the manufacturer's instructions. Several mutants from the PfPYL4-to-MpPYL1 reciprocal panel were created by a Gibson assembly-based strategy, using mutagenic primers and an

in-house reaction mixture, according to published protocols<sup>54</sup>.

**ABA-deficient Mutant phenotype suppression assay.** The *Arabidopsis thaliana* mutant *aba2-1* (Col-0 background) was used<sup>36</sup>. *A. thaliana* plants were grown in a growth chamber (Percival Scientific USA) under controlled light-intensity (70 to 100  $\mu\text{E}\cdot\text{m}^{-2}\cdot\text{s}^{-1}$ ) and temperature (20-22 °C) conditions. A long day diurnal period (16 h light/ 8 h dark) light period was used for plant propagation and a short-day period (10 h light/ 14 h dark) was used for ABA-deficient phenotype-suppression assays. Coding sequences of all tested PYLs were amplified with primers containing appropriate 5'-extensions and Gibson-assembled under the AtPYL4 promoter, into a pHeGHPB-derived vector. Mutated PYL variants were directly amplified from pBD-GAL4 or pET-28 vectors. The 35S promoter and a GFP-tag from the original plasmid were excluded from the resulting plasmid. Constructs were stably transformed into the *Arabidopsis* ABA-deficient mutant, *aba2-1* by floral dip. T1 seedlings were selected on MS agar media containing 15  $\mu\text{g}/\text{ml}$  glufosinate and transferred to soil in individual pots. Plants were grown for two months in growth chambers under short day conditions prior to analysis. Thermal images of the plants were taken at 10 AM, using a FLIR T630 camera (FLIR). Shoots were then separated and weighted to measure shoot biomass. Thermal images were subsequently analyzed using the FLIR Tools v5.2.15161.1001 software (FLIR). Each dot in box plots represents the means of 8 to 10 measurements of an individual plant.

## Quantification and statistical analysis

All data were statistically analyzed using JMP pro 12 statistical package (SAS Institute). Statistical parameters and methods of analysis are specified per each experiment in method details and in the respective figure legends. All box plots, bar graphs, and connecting lines were generated using Origin 8.1 Software.

## References

1. Ketterson, E.D., and Nolan, V. (1999). Adaptation, exaptation, and constraint: A hormonal perspective. *Am. Nat.* 154. <https://doi.org/10.1086/303280>.

2. Sun, Y., Pri-Tal, O., Michaeli, D., and Mosquna, A. (2020). Evolution of Abscisic Acid Signaling Module and Its Perception. *Front. Plant Sci.* *11*, 1–9. <https://doi.org/10.3389/fpls.2020.00934>.
3. Lüttge, U. (2020). Terrestrialization: The Conquest of Dry Land by Plants. In *Progress in Botany Vol. 83*, U. Lüttge, F. M. Cánovas, M.-C. Risueño, H. Pretzsch, and C. Leuschner, eds. (Springer), pp. 65–90. <https://doi.org/https://doi.org/10.1007/978-3-031-12782-3>.
4. Komatsu, K., Takezawa, D., and Sakata, Y. (2020). Decoding ABA and osmotic stress signalling in plants from an evolutionary point of view. *Plant Cell Environ.* *43*, 2894–2911. <https://doi.org/10.1111/pce.13869>.
5. Hsu, P.K., Dubeaux, G., Takahashi, Y., and Schroeder, J.I. (2021). Signaling mechanisms in abscisic acid-mediated stomatal closure. *Plant J.* *105*, 307–321. <https://doi.org/10.1111/tpj.15067>.
6. Ozturk, M., Turkyilmaz Unal, B., García-Caparrós, P., Khursheed, A., Gul, A., and Hasanuzzaman, M. (2021). Osmoregulation and its actions during the drought stress in plants. *Physiol. Plant.* *172*, 1321–1335. <https://doi.org/10.1111/ppl.13297>.
7. Nambara, E., Okamoto, M., Tatematsu, K., Yano, R., Seo, M., and Kamiya, Y. (2010). Abscisic acid and the control of seed dormancy and germination. *Seed Sci. Res.* *20*, 55–67. <https://doi.org/10.1017/S0960258510000012>.
8. Bianco, J., Garello, G., and Le Page-Degivry, M.T. (1997). De novo ABA synthesis and expression of seed dormancy in a gymnosperm: *Pseudotsuga menziesii*. *Plant Growth Regul.* *21*, 115–119. <https://doi.org/10.1023/A:1005707229810>.
9. Brodribb, T.J., and McAdam, S.A.M. (2013). Abscisic acid mediates a divergence in the drought response of two conifers. *Plant Physiol.* *162*, 1370–1377. <https://doi.org/10.1104/pp.113.217877>.
10. McAdam, S.A.M., and Brodribb, T.J. (2012). Fern and lycophyte guard cells do not respond to endogenous abscisic acid. *Plant Cell* *24*, 1510–1521. <https://doi.org/10.1105/tpc.112.096404>.
11. Takezawa, D., Komatsu, K., and Sakata, Y. (2011). ABA in bryophytes: How a universal growth regulator in life became a plant hormone? *J. Plant Res.* *124*, 437–453. <https://doi.org/10.1007/s10265-011-0410-5>.
12. Proctor, M.C.F., Oliver, M.J., Wood, A.J., Alpert, P., Stark, L.R., Cleavitt, N.L., and Mishler, B.D. (2007). Desiccation-tolerance in bryophytes: A review. *Bryologist* *110*, 595–621. [https://doi.org/10.1639/0007-2745\(2007\)110\[595:DIBAR\]2.0.CO;2](https://doi.org/10.1639/0007-2745(2007)110[595:DIBAR]2.0.CO;2).
13. Eklund, D.M., Kanei, M., Flores-Sandoval, E., Ishizaki, K., Nishihama, R., Kohchi, T., Lagercrantz, U., Bhalerao, R.P., Sakata, Y., and Bowman, J.L. (2018). An Evolutionarily Conserved Abscisic Acid Signaling Pathway Regulates Dormancy in the Liverwort *Marchantia polymorpha*. *Curr. Biol.* *28*, 3691–3699.e3. <https://doi.org/10.1016/j.cub.2018.10.018>.
14. Vesty, E.F., Saidi, Y., Moody, L.A., Holloway, D., Whitbread, A., Needs, S., Choudhary, A., Burns, B., McLeod, D., Bradshaw, S.J., et al. (2016). The decision to germinate is regulated by divergent molecular networks in spores and seeds. *New Phytol.* *211*, 952–966. <https://doi.org/10.1111/nph.14018>.
15. Arif, M.A., Hiss, M., Tomek, M., Busch, H., Meyberg, R., Tintelnot, S., Reski, R., Rensing, S.A., and

- Frank, W. (2019). ABA-induced vegetative diaspore formation in *Physcomitrella patens*. *Front. Plant Sci.* *10*, 1–18. <https://doi.org/10.3389/fpls.2019.00315>.
16. Hauser, F., Waadt, R., and Schroeder, J.I. (2011). Evolution of abscisic acid synthesis and signaling mechanisms. *Curr. Biol.* *21*, R346–R355. <https://doi.org/10.1016/j.cub.2011.03.015>.
  17. Ma, Y., Szostkiewicz, I., Korte, A., Moes, D., Yang, Y., Christmann, A., and Grill, E. (2009). Regulators of PP2C phosphatase activity function as abscisic acid sensors. *Science* (80- ). *324*, 1064–1068.
  18. Park, S.S.-Y., Fung, P., Nishimura, N., Jensen, D.R., Fujii, H., Zhao, Y., Lumba, S., Santiago, J., Rodrigues, A., Chow, T.F.T. -f. F., et al. (2009). Abscisic Acid Inhibits Type 2C Protein Phosphatases via the PYR/PYL Family of START Proteins. *Science* (80- ). *324*, 1068–1069.
  19. Cutler, S.R., Rodriguez, P.L., Finkelstein, R.R., and Abrams, S.R. (2010). Abscisic acid: Emergence of a core signaling network <https://doi.org/10.1146/annurev-arplant-042809-112122>.
  20. Szostkiewicz, I., Richter, K., Kepka, M., Demmel, S., Ma, Y., Korte, A., Assaad, F.F., Christmann, A., and Grill, E. (2010). Closely related receptor complexes differ in their ABA selectivity and sensitivity. *Plant J.* *61*, 25–35. <https://doi.org/10.1111/j.1365-313X.2009.04025.x>.
  21. Ruschhaupt, M., Mergner, J., Mucha, S., Papacek, M., Doch, I., Tischer, S. V., Hemmler, D., Chiasson, D., Edel, K.H., Kudla, J., et al. (2019). Rebuilding core abscisic acid signaling pathways of *Arabidopsis* in yeast. *EMBO J.* *38*, 1–14. <https://doi.org/10.15252/emboj.2019101859>.
  22. Wickett, N.J., Mirarab, S., Nguyen, N., Warnow, T., Carpenter, E., Matasci, N., Ayyampalayam, S., Barker, M.S., Burleigh, J.G., Gitzendanner, M.A., et al. (2014). Phylotranscriptomic analysis of the origin and early diversification of land plants. *Proc. Natl. Acad. Sci. U. S. A.* *111*, E4859–E4868. <https://doi.org/10.1073/pnas.1323926111>.
  23. Morris, J.L., Puttick, M.N., Clark, J.W., Edwards, D., Kenrick, P., Pressel, S., Wellman, C.H., Yang, Z., Schneider, H., and Donoghue, P.C.J. (2018). The timescale of early land plant evolution. *Proc. Natl. Acad. Sci. U. S. A.* *115*, E2274–E2283. <https://doi.org/10.1073/pnas.1719588115>.
  24. De Vries, J., Curtis, B.A., Gould, S.B., and Archibald, J.M. (2018). Embryophyte stress signaling evolved in the algal progenitors of land plants. *Proc. Natl. Acad. Sci. U. S. A.* *115*, E3471–E3480. <https://doi.org/10.1073/pnas.1719230115>.
  25. Feng, X., Zheng, J., Irisarri, I., Yu, H., Zheng, B., Ali, Z., de Vries, S., Keller, J., Fürst-Jansen, J.M.R., Dadras, A., et al. (2024). Genomes of multicellular algal sisters to land plants illuminate signaling network evolution. *Nat. Genet.* *56*, 1018–1031. <https://doi.org/10.1038/s41588-024-01737-3>.
  26. Sun, Y., Harpazi, B., Wijerathna-Yapa, A., Merilo, E., de Vries, J., Michaeli, D., Gal, M., Cuming, A.C., Kollist, H., and Mosquna, A. (2019). A ligand-independent origin of abscisic acid perception. *Proc. Natl. Acad. Sci. U. S. A.* *116*, 24892–24899. <https://doi.org/10.1073/pnas.1914480116>.
  27. Dupeux, F., Santiago, J., Betz, K., Twycross, J., Park, S.Y., Rodriguez, L., Gonzalez-Guzman, M., Jensen, M.R., Krasnogor, N., Blackledge, M., et al. (2011). A thermodynamic switch modulates abscisic acid receptor sensitivity. *EMBO J.* *30*, 4171–4184. <https://doi.org/10.1038/emboj.2011.294>.

28. Hao, Q., Yin, P., Li, W., Wang, L., Yan, C., Lin, Z., Wu, J.Z., Wang, J., Yan, S.F., and Yan, N. (2011). The Molecular Basis of ABA-Independent Inhibition of PP2Cs by a Subclass of PYL Proteins. *Mol. Cell* 42, 662–672. <https://doi.org/10.1016/j.molcel.2011.05.011>.
29. Fürst-Jansen, J.M.R., De Vries, S., De Vries, J., and De Vries, J. (2020). Evo-physio: On stress responses and the earliest land plants. *J. Exp. Bot.* 71, 3254–3269. <https://doi.org/10.1093/jxb/eraa007>.
30. Zhao, M., Li, Q., Chen, Z., Lv, Q., Bao, F., Wang, X., and He, Y. (2018). Regulatory mechanism of ABA and ABI3 on vegetative development in the moss *Physcomitrella patens*. *Int. J. Mol. Sci.* 19, 1–19. <https://doi.org/10.3390/ijms19092728>.
31. Garland, T., Downs, C.J., and Ives, A.R. (2022). Trade-offs (And constraints) in organismal biology. *Physiol. Biochem. Zool.* 95, 82–112. <https://doi.org/10.1086/717897>.
32. Liu, Y., Johnson, M.G., Cox, C.J., Medina, R., Devos, N., Vanderpoorten, A., Hedenäs, L., Bell, N.E., Shevock, J.R., Aguero, B., et al. (2019). Resolution of the ordinal phylogeny of mosses using targeted exons from organellar and nuclear genomes. *Nat. Commun.* 10. <https://doi.org/10.1038/s41467-019-09454-w>.
33. Mosquna, A., Peterson, F.C., Park, S.Y., Lozano-Juste, J., Volkman, B.F., and Cutler, S.R. (2011). Potent and selective activation of abscisic acid receptors in vivo by mutational stabilization of their agonist-bound conformation. *Proc. Natl. Acad. Sci. U. S. A.* 108, 20838–20843. <https://doi.org/10.1073/pnas.1112838108>.
34. Pri-Tal, O., Sun, Y., Dadras, A., Fürst-Jansen, J.M.R., Zimran, G., Michaeli, D., Wijerathna-Yapa, A., Shpilman, M., Merilo, E., Yarmolinsky, D., et al. (2024). Constitutive activation of ABA receptors in *Arabidopsis* reveals unique regulatory circuitries. *New Phytol.* 241, 703–714. <https://doi.org/10.1111/nph.19363>.
35. Schaefer, D., Zryd, J.P., Knight, C.D., and Cove, D.J. (1991). Stable transformation of the moss *Physcomitrella patens*. *MGG Mol. Gen. Genet.* 226, 418–424. <https://doi.org/10.1007/BF00260654>.
36. Léon-Kloosterziel, K.M., Gil, M.A., Ruijs, G.J., Jacobsen, S.E., Olszewski, N.E., Schwartz, S.H., Zeevaart, J.A.D., and Koornneef, M. (1996). Isolation and characterization of abscisic acid-deficient *Arabidopsis* mutants at two new loci. *Plant J.* 10, 655–661. <https://doi.org/10.1046/j.1365-313X.1996.10040655.x>.
37. Perroud, P.F., Haas, F.B., Hiss, M., Ullrich, K.K., Alboresi, A., Amirebrahimi, M., Barry, K., Bassi, R., Bonhomme, S., Chen, H., et al. (2018). The *Physcomitrella patens* gene atlas project: large-scale RNA-seq based expression data. *Plant J.* 95, 168–182. <https://doi.org/10.1111/tpj.13940>.
38. Knight, C.D., Sehgal, A., Atwal, K., Wallace, J.C., Cove, D.J., Coates, D., Quatrano, R.S., Bahadur, S., Stockley, P.G., and Cuming, A.C. (1995). Molecular responses to abscisic acid and stress are conserved between moss and cereals. *Plant Cell* 7, 499–506. <https://doi.org/10.2307/3870110>.
39. Mcelroy, D., Wanggen, Z., Jun, C., and Ray, W. (1990). Isolation of an Efficient Actin Promoter for Use in Rice Transformation. *Plant Cell* 2, 163–171.
40. Katoh, K., and Standley, D.M. (2013). MAFFT multiple sequence alignment software version 7:

- Improvements in performance and usability. *Mol. Biol. Evol.* *30*, 772–780.  
<https://doi.org/10.1093/molbev/mst010>.
41. Nguyen, L.T., Schmidt, H.A., Von Haeseler, A., and Minh, B.Q. (2015). IQ-TREE: A fast and effective stochastic algorithm for estimating maximum-likelihood phylogenies. *Mol. Biol. Evol.* *32*, 268–274.  
<https://doi.org/10.1093/molbev/msu300>.
  42. Kalyaanamoorthy, S., Minh, B.Q., Wong, T.K.F., Von Haeseler, A., and Jermini, L.S. (2017). ModelFinder: Fast model selection for accurate phylogenetic estimates. *Nat. Methods* *14*, 587–589. <https://doi.org/10.1038/nmeth.4285>.
  43. Concordet, J.P., and Haeussler, M. (2018). CRISPOR: Intuitive guide selection for CRISPR/Cas9 genome editing experiments and screens. *Nucleic Acids Res.* *46*, W242–W245.  
<https://doi.org/10.1093/nar/gky354>.
  44. Fauser, F., Schiml, S., and Puchta, H. (2014). Both CRISPR/Cas-based nucleases and nickases can be used efficiently for genome engineering in *Arabidopsis thaliana*. *Plant J.* *79*, 348–359.  
<https://doi.org/10.1111/tpj.12554>.
  45. Kamisugi, Y., Cuming, A.C., and Cove, D.J. (2005). Parameters determining the efficiency of gene targeting in the moss *Physcomitrella patens*. *Nucleic Acids Res.* *33*, 1–10.  
<https://doi.org/10.1093/nar/gni172>.
  46. Lopez-Obando, M., Hoffmann, B., Géry, C., Guyon-Debast, A., Téoulé, E., Rameau, C., Bonhomme, S., and Nogué, F. (2016). Simple and efficient targeting of multiple genes through CRISPR-Cas9 in *Physcomitrella patens*. *G3 Genes, Genomes, Genet.* *6*, 3647–3653.  
<https://doi.org/10.1534/g3.116.033266>.
  47. Stevenson, S.R., Kamisugi, Y., Trinh, C.H., Schmutz, J., Jenkins, J.W., Grimwood, J., Muchero, W., Tuskan, G.A., Rensing, S.A., Lang, D., et al. (2016). Genetic analysis of *Physcomitrella patens* identifies ABSCISIC ACID NON-RESPONSIVE, a regulator of ABA responses unique to basal land plants and required for desiccation tolerance. *Plant Cell* *28*, 1310–1327.  
<https://doi.org/10.1105/tpc.16.00091>.
  48. Kamisugi, Y., Schaefer, D.G., Kozak, J., Charlot, F., Vrielynck, N., Holá, M., Angelis, K.J., Cuming, A.C., and Nogué, F. (2012). MRE11 and RAD50, but not NBS1, are essential for gene targeting in the moss *Physcomitrella patens*. *Nucleic Acids Res.* *40*, 3496–3510.  
<https://doi.org/10.1093/nar/gkr1272>.
  49. Marcotte, W.R., Russell, S.H., and Quatrano, R.S. (1989). Abscisic acid-responsive sequences from the em gene of wheat. *Plant Cell* *1*, 969–976. <https://doi.org/10.1105/tpc.1.10.969>.
  50. Jefferson, R.A., Kavanagh, T.A., and Bevan, M.W. (1987). GUS fusions: beta-glucuronidase as a sensitive and versatile gene fusion marker in higher plants. *EMBO J.* *6*, 3901–3907.  
<https://doi.org/10.1002/j.1460-2075.1987.tb02730.x>.
  51. Saez, A., Rodrigues, A., Santiago, J., Rubio, S., and Rodriguez, P.L. (2008). HAB1-SWI3B interaction reveals a link between abscisic acid signaling and putative SWI/SNF chromatin-remodeling complexes in *Arabidopsis*. *Plant Cell* *20*, 2972–2988. <https://doi.org/10.1105/tpc.107.056705>.
  52. Okamoto, M., Peterson, F.C., Defries, A., Park, S.Y., Endo, A., Nambara, E., Volkman, B.F., and

Cutler, S.R. (2013). Activation of dimeric ABA receptors elicits guard cell closure, ABA-regulated gene expression, and drought tolerance. *Proc. Natl. Acad. Sci. U. S. A.* *110*, 12132–12137. <https://doi.org/10.1073/pnas.1305919110>.

53. Mosquna, a., Peterson, F.C., Park, S.-Y., Lozano-Juste, J., Volkman, B.F., and Cutler, S.R. (2011). Potent and selective activation of abscisic acid receptors in vivo by mutational stabilization of their agonist-bound conformation. *Proc. Natl. Acad. Sci.* *108*, 20838–20843. <https://doi.org/10.1073/pnas.1112838108>.
54. Avilan, L. (2023). Assembling Multiple Fragments: The Gibson Assembly. In *DNA Manipulation and Analysis*, G. Scarlett, ed. (Humana Press), pp. 45–54. <https://doi.org/10.1007/978-1-0716-3004-4>.

# Figures and Tables

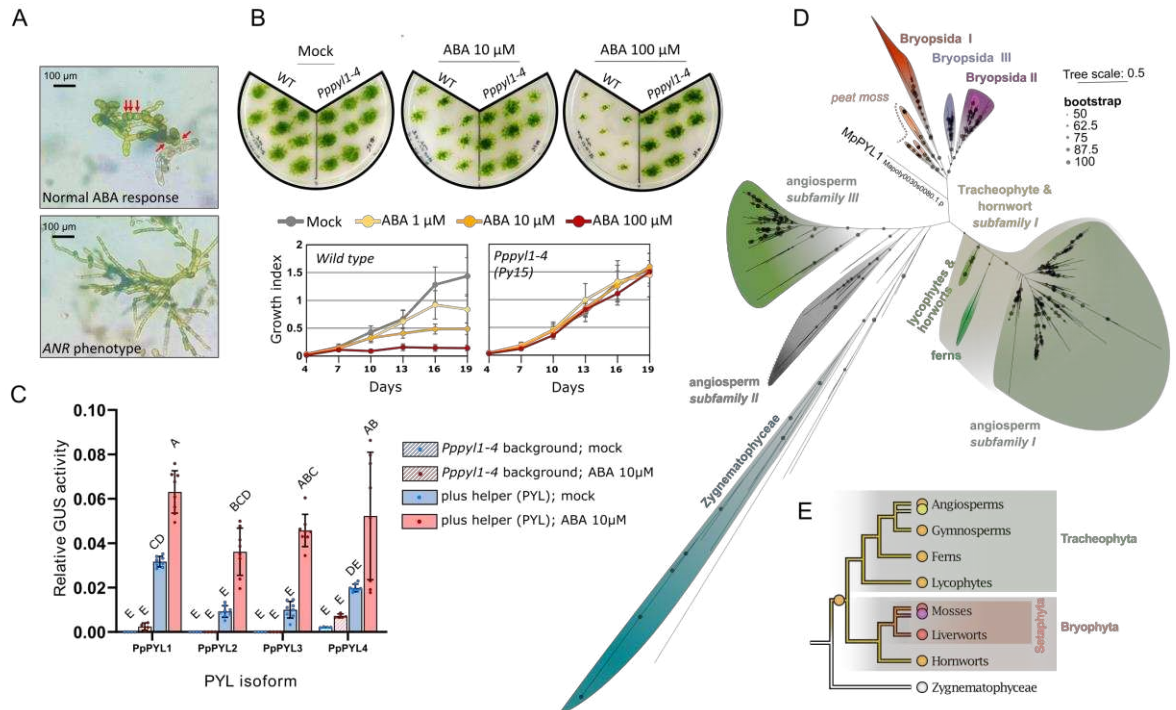


**Figure 1. Independent radiation of PYL receptors gave rise to Abscisic acid perception in mosses.** (A-C) Knockout of four PYL genes is sufficient to nullify ABA responsiveness in the model moss *Physcomitrium patens*. CRISPR cassettes targeting the five putative *P. patens* PYLs were introduced, and lines displaying a clear ABA non-responsive (“ANR”) phenotype<sup>47</sup> were selected for further characterization. (A) Representative images of ABA-responsive (top) and non-responsive (bottom) phenotypes, taken 5 days following transfer to an ABA-containing medium. ABA-responsive plants are recognizable by the formation of small, thick-walled “brood cells” (arrowed), while ANR plants display unrestricted growth of protonemal tissue on the same medium. (B) Growth curves of wild type *P. patens* and a multiple PYL-knockout line (*Py15*). Petri plates were photographed at 3-day intervals between days 4 and 19 following inoculation with protonemal homogenate tissue. Photos taken 16 days post inoculation are shown below, with genotypes and ABA concentrations indicated. The “growth index” was calculated as (plant pixel area)/(mean pixel area of reference spots) and error bars indicate standard deviation (n=8). Two additional ANR lines (*Py7* and *Py24*) were similarly unaffected by saturating levels of ABA (Figure S1). All Three of these lines - *Py7*, *Py24* and *Py15*, were genetically examined and all contained loss-of-function alleles in *PpPYLs* 1-4 (Pp3c26\_15240; Pp3c13\_7110; Pp3c7\_26290; Pp3c9\_19760). Disruption of *PpPYL5* (Pp3c3\_660) was only confirmed in *Py15* and review of latest available transcriptional data revealed it is likely a pseudogene (Table S1). For detailed description of genotypes see related supplemental Table S1. (C) Restoration of ABA-dependent transcription in *PpPYL1-4* protoplasts, by native isoforms. In each experiment, protoplast-suspensions derived from line *Py15* were transfected with two plasmids carrying an ABA-reporter system and with a third 'helper-plasmid' harboring one of the tested PYLs. Each experiment included a parallel protoplast suspension not transfected with a helper-plasmid, as control. Both suspensions were incubated with- or without ABA (10 μM) for 24 hours, harvested and lysed to determine GUS and Luciferase activities. Relative GUS activity was obtained by

dividing the yield of the  $\beta$ -glucuronidase reaction product 4-methyl umbelliferone by the luciferase luminescence yield, in each reaction mix. Connecting letters indicate non-significant difference according to Tukey HSD analysis (Adjusted DF=80;  $q=3.5374$ ) implemented to a Standard Least Squares model that includes all levels and considers the nesting of 'Helper' and 'ABA' treatments plus their interaction within 'PYL-isoform' (adjusted  $R^2=0.82$ ; whole model  $prob>F$  smaller than 0.001;  $n=8$  and  $n=4$  for 'Helper' and 'No helper' treatments, respectively). **(D)** A maximum likelihood phylogeny of 536 PYL homologs computed using the best fit model (according to Bayesian Information Criterion) for protein evolution JTT+G4 and 500 non-parametric bootstrap pseudoreplicates; Scale bar for phylogeny is 0.5 expected substitutions per site. **(E)** Simplified cladogram of land plant evolution with the diversification of PYL homologs indicated by colored dots.

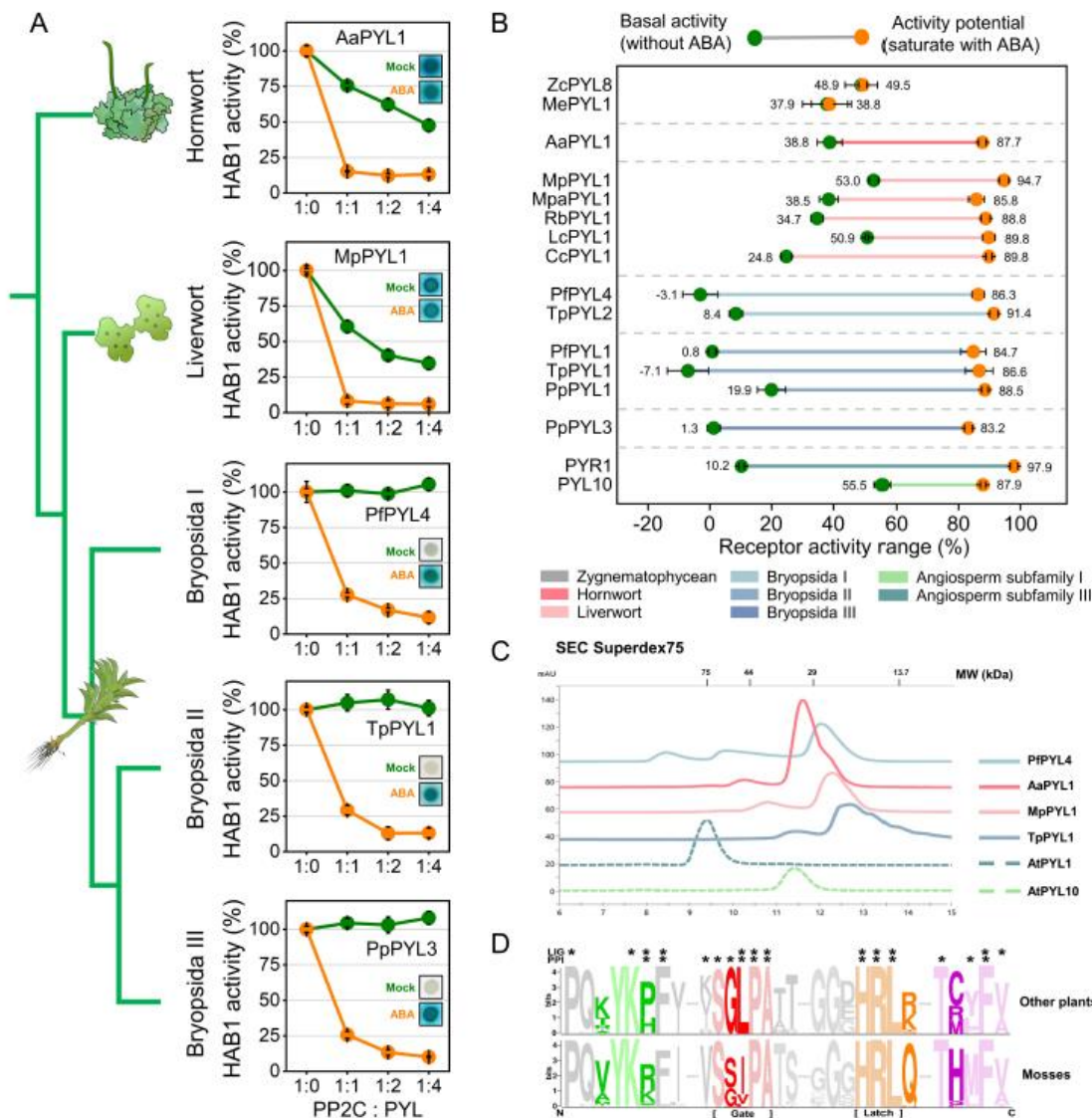
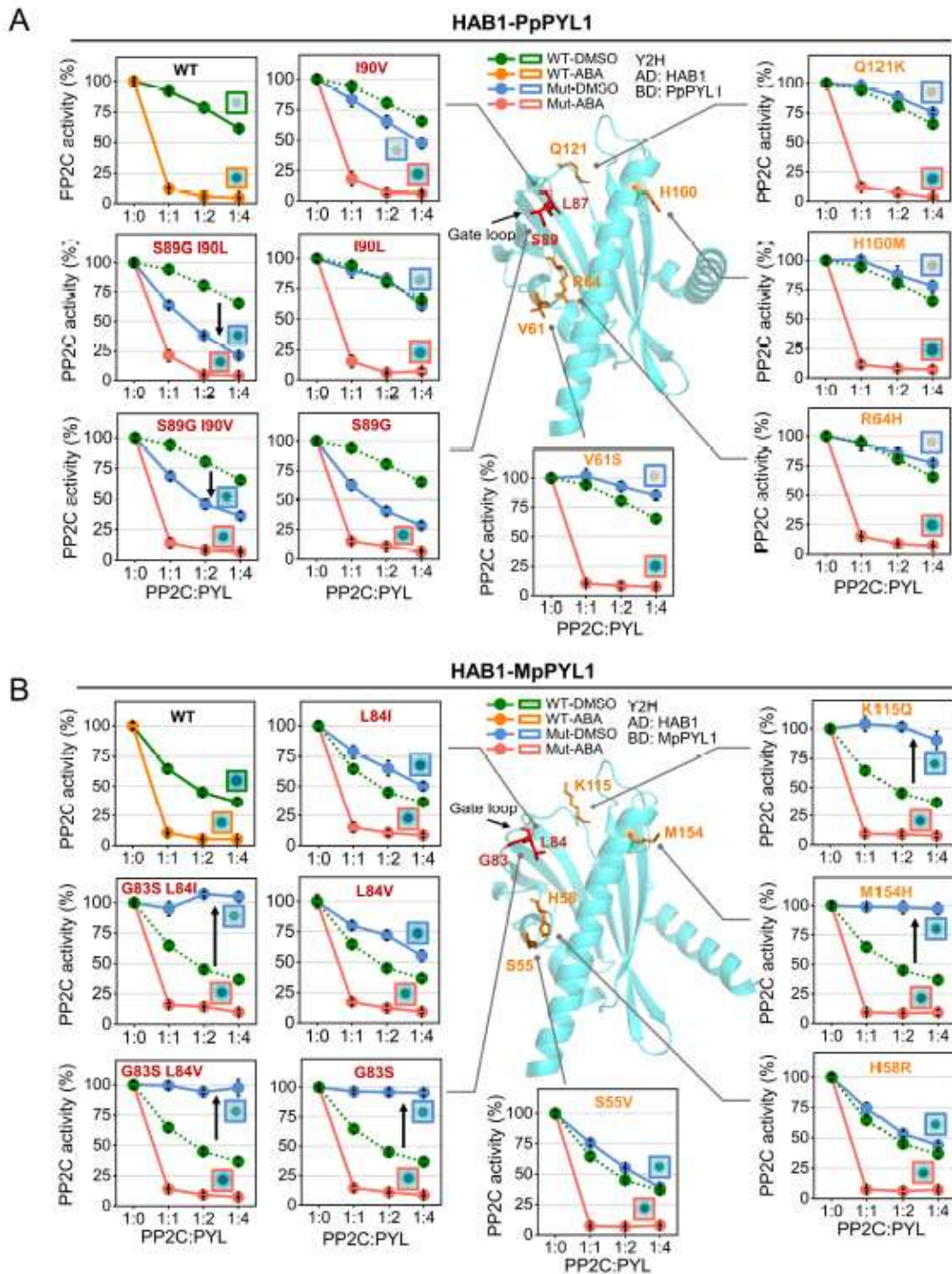


**Figure 2. ABA receptors from all Bryophytina-specific subfamilies display a high degree of ABA-dependency despite being monomeric. (A)** HAB1-inhibition by representative ABA receptors from hornworts, liverworts, and three Bryopsida subfamilies. Recombinant 6×His-PYLs were expressed in *E. coli*, purified, and used in PP2C inhibition assays. Reactions were performed with 0.3 μM HAB1 and varying concentrations of PYL (0, 0.3, 0.6, 1.2 μM) in the absence (green) or presence (orange) of 10 μM ABA. PP2C activity is expressed as a percentage of PP2C activity without any receptor. Error bars indicate SD for 3 technical repeats. PYL-PP2C interaction tested by yeast two-hybrid is shown by insert boxes. PYL proteins were constructed as binding-domain (BD) fusions and tested for interaction with activation-domain (AD) fused HAB1 in the presence of 10 μM ABA (bottom) or 0.1% DMSO as mock (top). **(B)** Dynamic response range of receptor activity. The green dot indicates receptor activity, captured at a PYL:PP2C ratio of 2:1 without ABA (see also Figure S2). The orange dot indicated receptor activity potential, captured at the same PYL/PP2C ratio when saturated with 10 μM ABA. Average values of three repeats are shown beside the dots, and error bars indicate SD. **(C)** Size exclusion chromatography elution

profiles of the monomeric AtPYL10 and the dimeric AtPYL1 (dashed lines) along the receptors TpPYL1, MpPYL1, AaPYL1 and PfPYL4 (solid lines). Molecular marker (top) derives from an SEC elution profile of a protein mix composed of conalbumin (MW = 75 kDa), ovoalbumin (MW = 44 kDa), carbonic anhydrase (MW = 29 kDa) and RNase (MW = 13.7 kDa). **(D)** Consensus logos of ABA receptors. The above sequence was generated by 315 ABA receptors from all phyla, excluding mosses, while the bottom sequence was generated by 134 mosses receptors. Asterisks indicate ABA (LIG) or PP2C (PPI) interaction. Four ligand- and PP2C-interacting domains that contain divergent residues are colored as follows: green – internal helix and adjacent loops; red – gate loop; orange – latch loop; purple – C-terminal helix and adjacent sequence. See also Figure S4. Genes prefixes designate species of origin as follows : Aa – *Anthoceros agrestis*; At - *Arabidopsis thaliana*; Cc - *Conocephalum conicum*; Lc - *Lunularia cruciata*; Me - *Mesotaenium endlicherianum*; Mp - *Marchantia polymorpha*; Mpa - *Marchantia paleacea*; Pf - *Philonotis fontana*; Pp – *Physcomitrium patens*; Rb - *Riccia berychiana*; Tp - *Tetraphis pellucida*; Zc - *Zygnema circumcarinatum*.



activity in the presence of mutated PYL proteins; with red and blue lines designating reactions with and without 10  $\mu$ M ABA, respectively. In both sections, the ligand-free activity of the wild type receptor is superimposed on all other charts for ease of comparison (green dashed lines). Error bars indicate SD for three repeats. For each PYL variant, insert boxes show Y2H assays for PYL-HAB1 interaction, with or without ABA. Locations of gate and PP2C interface residues are mapped on PpPYL1 or MpPYL1 model predicted by AlphaFold. See also Figure S6 for complementary analysis.

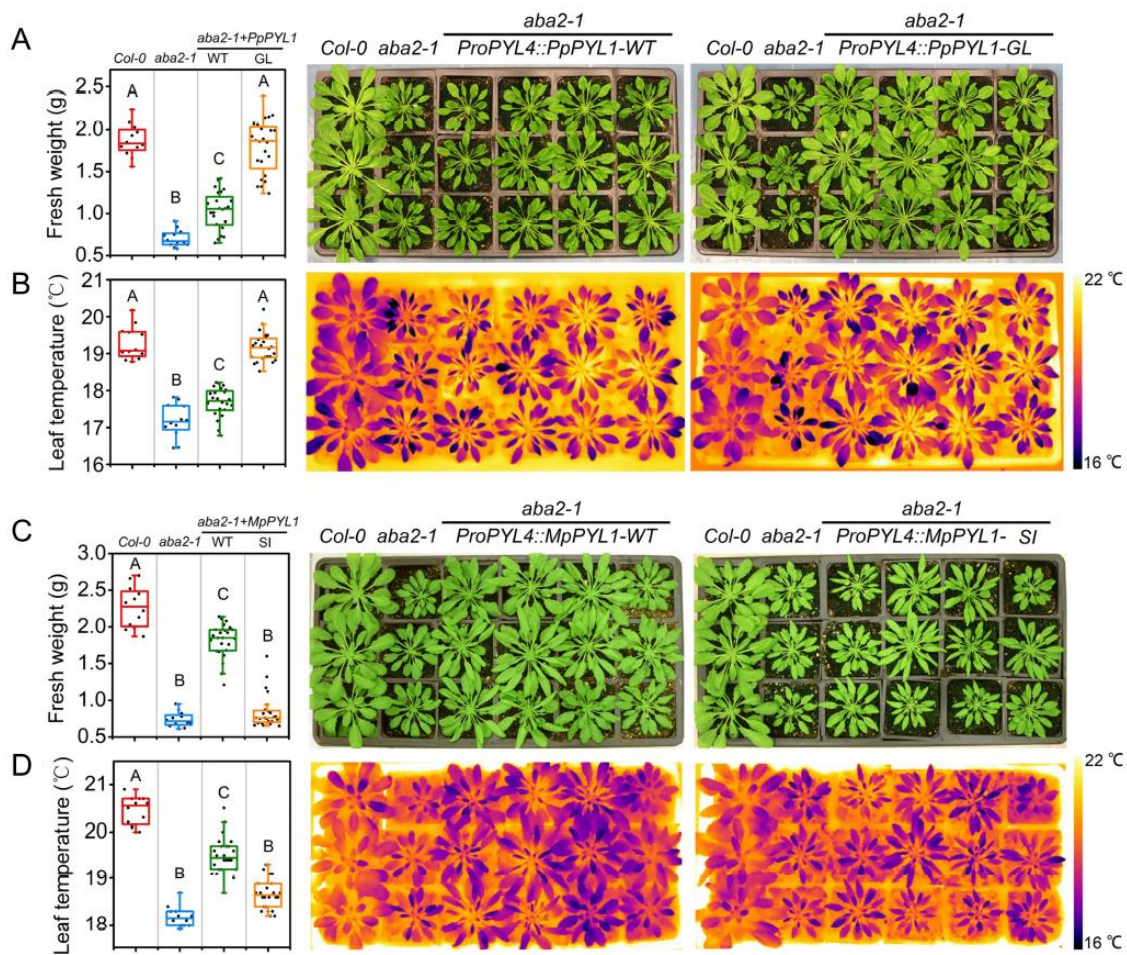


**Figure 4. Gate mutations are sufficient to alter receptor basal signaling activity *in planta*.** Wild-type and mutated PYLs were expressed under the control of the *AtPYL4* promoter in the ABA-deficient mutant *aba2-1*. Independent T1 plants were selected based on glufosinate-resistance and transplanted to soil alongside the *Col-0* and *aba2-1* controls. **(A and C)** Phenotype and fresh weight of *Col-0*, *aba2-1*, and *aba2-1* mutants expressing wild-type and gate-mutated versions of PpPYL1 **(A)** or MpPYL1 **(C)**. **(B and D)** Thermograph and leaf temperature of *Col-0*, *aba2-1*, and *aba2-1* mutants expressing wild-type and gate-mutated versions of PpPYL1 **(B)** or MpPYL1 **(D)**. Photographs were taken after 6 weeks of growth under short-day conditions (8/16 day/night). Different letters indicate statistically significant differences (Tukey HSD test,  $df = 3$  [ $P < 0.01$ ], for transgenic plants,  $n = 24$ ; for *Col-0* and *aba2-1*,  $n = 12$ ). See also Figure S6 for com.

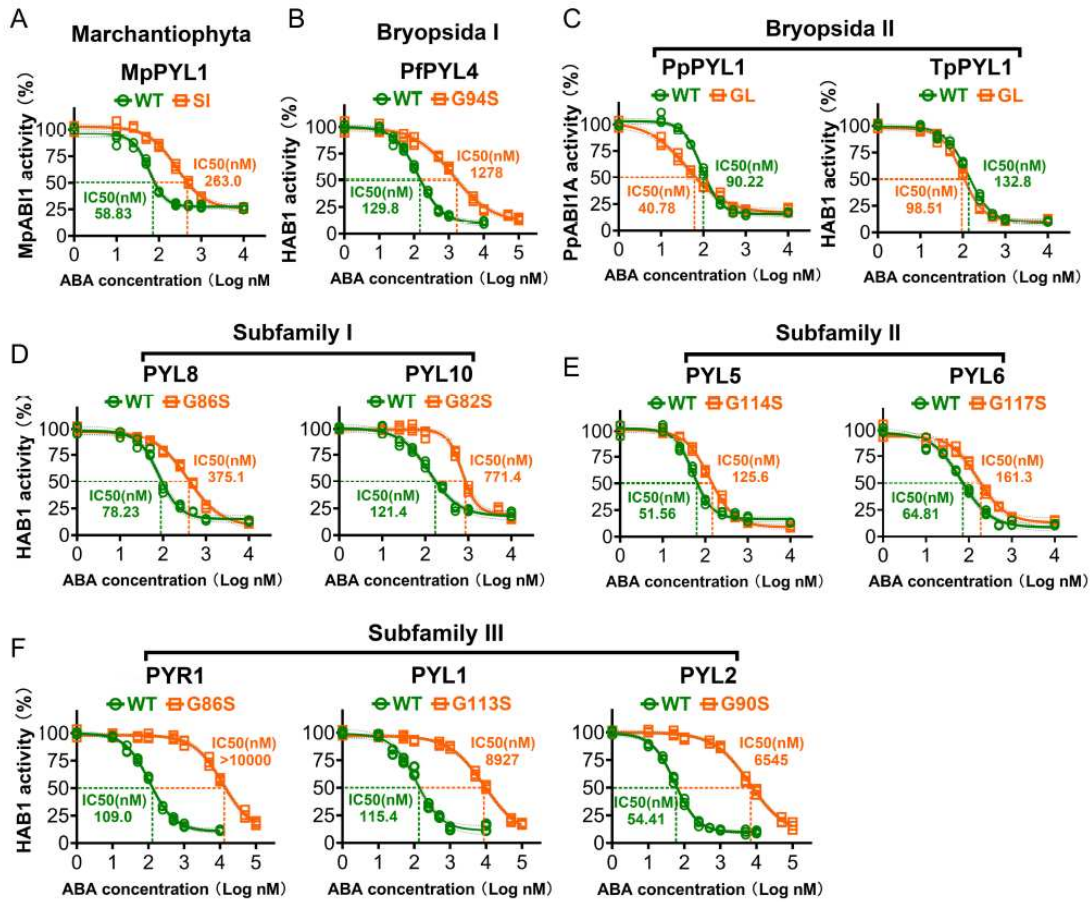


**Figure 5. Glycine to Serine substitution compromises ABA-triggered PP2C inhibition in a subfamily-dependent manner.** Recombinant 6×His-PP2C activity was measured in the presence of wild-type (green) and gate-mutated versions (orange) of 6×His-PYLs on a series of ABA concentrations. The reactions contained 0.3 μM 6×His-HAB1 and 0.6 μM of the recombinant receptor. Phosphatase activity was calculated using three technical replicates and error bars indicate SD. IC50 values are indicated numerically.

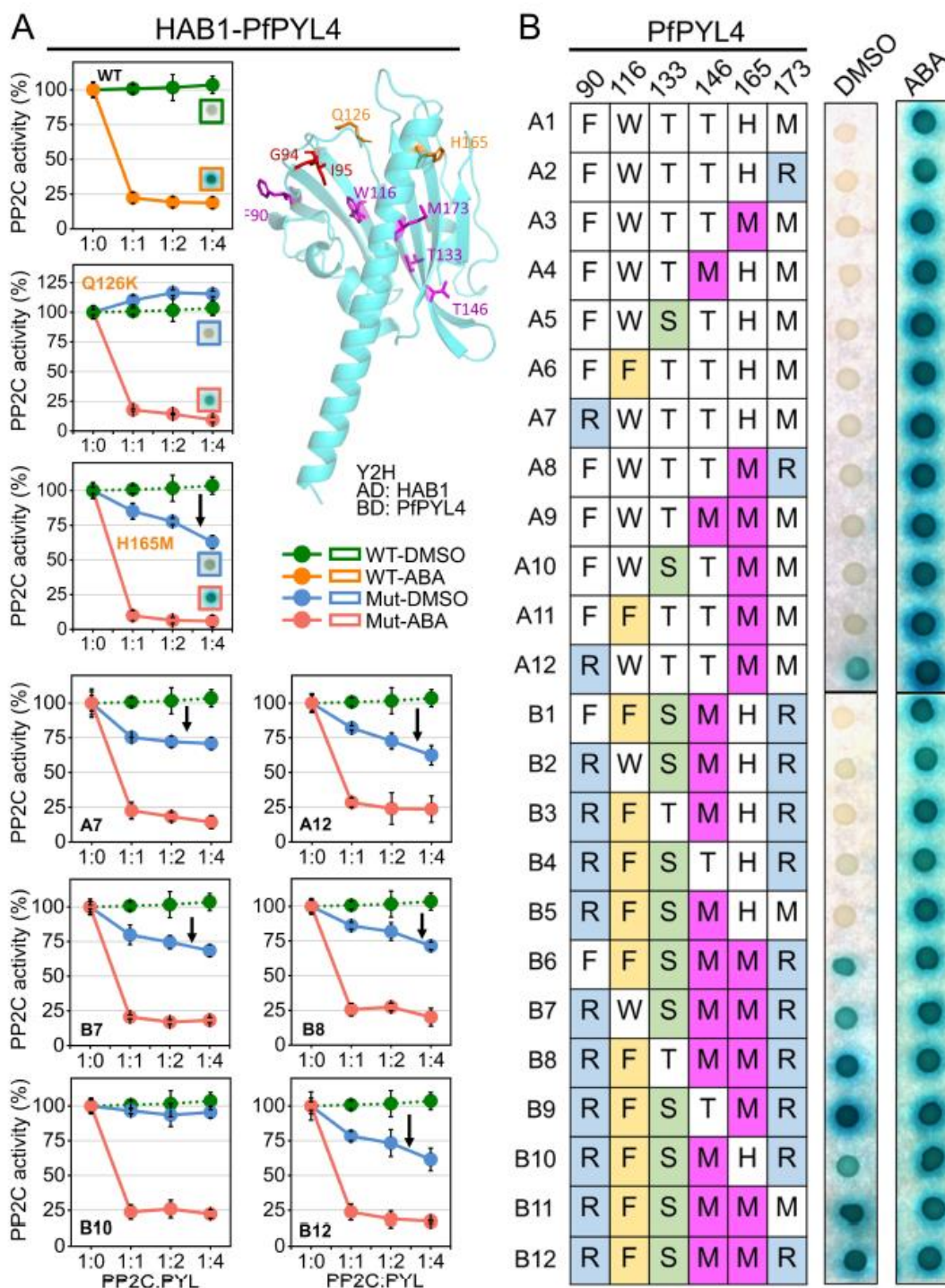


**Figure 6. Multiple amino acid variations contribute to the high ligand-dependent activity of the Bryopsida subfamily I receptor PfPYL4.** (A) HAB1 inhibition by wild-type or mutated PfPYL4. The top chart shows HAB1 activity in the presence of wild-type PfPYL4; with reactions containing 10  $\mu$ M ABA represented by orange lines and reactions in the absence of ABA represented by green lines. All other charts show HAB1 activity in the presence of PfPYL4 mutants; with red and blue lines designating

reactions with and without 10  $\mu$ M ABA, respectively. The ligand-free activity of wild-type PfpYL4 is superimposed on all other charts for ease of comparison (green dashed lines). PP2C activity is expressed as a percentage of the activity of PP2C in the absence of the receptor. Error bars indicate SD for three repeats. Insert boxes show Y2H assays for PYL-HAB1 interaction with or without 10  $\mu$ M ABA. Locations of gate and PP2C interface residues are mapped on PfpYL4 model predicted by Alphafold. **(B)** Y2H assay of a PfpYL4 mutant panel for basal and ABA-dependent interaction with HAB1. The genotype of each PfpYL4 variant is indicated in the table to the left. See also Figure S8.

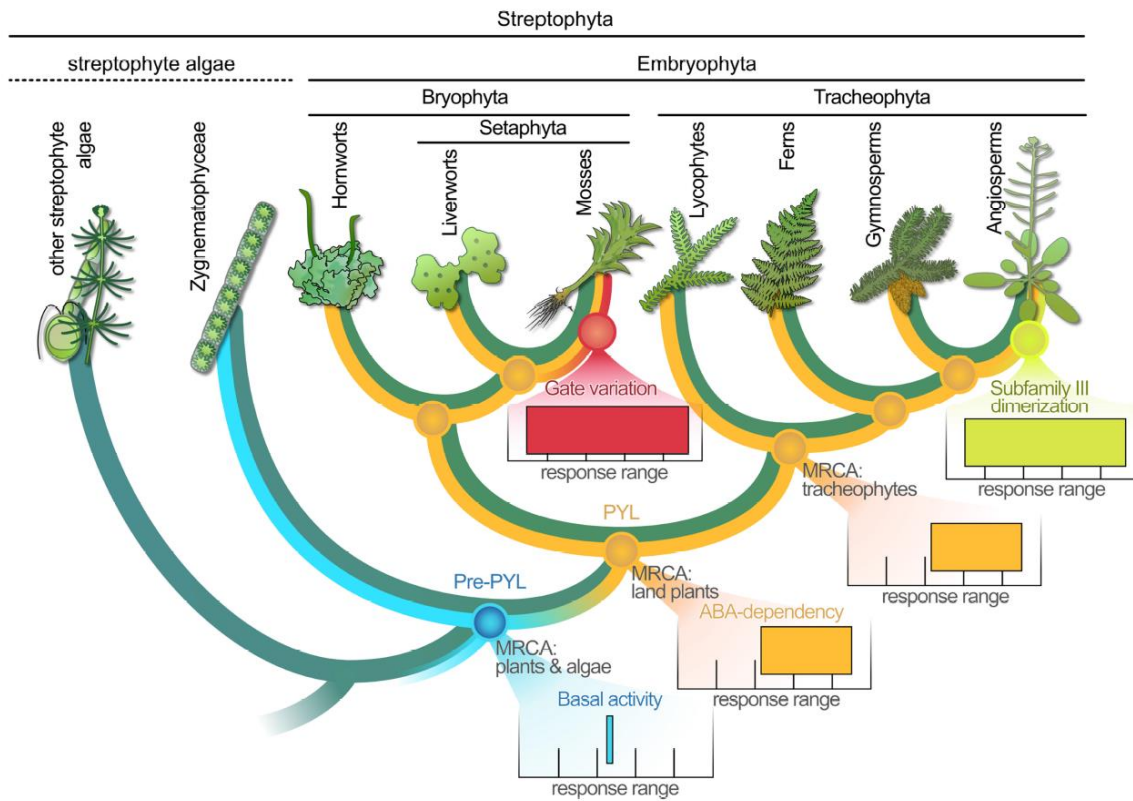


**Figure 7. Convergence of abscisic acid receptors towards increased ABA-dependency across the deep divergence between mosses and angiosperms.** Archetypal dynamic ranges of ABA perception and downstream signaling by PYL receptors along the green lineage.